THE PENNSYLVANIA
STATE UNIVERSITY

IONOSPHERIC RESEARCH

Scientific Report No. 360

CALIBRATIONS OF THE ARECIBO FACILITY FOR IONOSPHERIC STUDIES

by
D. E. BARAN
July 30, 1970

IONOSPHERE RESEARCH LABORATORY

University Park, Pennsylvania NASA Grant NGL-39-009-003

Ionospheric Research

NASA Grant NGL 39-009-003

Scientific Report

on

"Calibrations of the Arecibo Facility for Ionospheric Studies"

by

D. E. Baran

July 30, 1970

Scientific Report No. 360

Ionosphere Research Laboratory

Submitted by: John S. Nisbet

John S. Nisbet, Professor of Electrical Engineering
Project Supervisor

Approved by: A. H. Waynick

A. H. Waynick, Director
Ionosphere Research Laboratory

The Pennsylvania State University

College of Engineering

Department of Electrical Engineering

TABLE OF CONTENTS

ACKNOWLEDGMENTS

I would like to thank Drs. H. C. Carlson, A. J. Ferraro, L. M. LaLonde, S. R. Laxpati, J. R. Mentzer, J. S. Nisbet, J. Sutton, and L. S. Wagner, and also D. Albino, J. E. Binns, R. L. Divany, M. A. Feyjoo, F. S. Harris, and the staffs of the Ionosphere Research Laboratory and the Arecibo Observatory for their advice and assistance in this work. This work was supported by NASA grant NGL 39-009-003. The Arecibo Observatory is operated by Cornell University with the support of the Advanced Research Projects Agency and the National Science Foundation under contract with the Air Force Office of Scientific Research.

ABSTRACT

This study is concerned with the calibration of the Arecibo facility for ionospheric studies. Investigations of measured parameters were generally confined to the area of the F2 peak. Of primary interest were the day to night backscatter gain fluctuations.

Ten standard ionospheric experiments along with several variations of these were employed in order to obtain statistical data with regard to the parameters of the ionosphere radar equation. Temperature measurements on the antenna structure and radio astronomy measurements were made to determine the cause of the gain fluctuations. In addition, theoretical studies of gain variations resulting from temperature changes were made.

Results of the study showed that the backscatter gain variations are caused by distortion of the reflector surface which in turn is caused by temperature fluctuations. The accuracies of the radar equation parameters were determined and are given in the conclusions.

CHAPTER I

INTRODUCTION

1.1 General Statement of the Problem

At the Arecibo Ionospheric Observatory electron densities and electron and ion temperatures are measured as a function of altitude. It is of importance to the investigations which use these data that they be as accurate as possible. As a result of this, the present study is aimed at calibrating the Arecibo system.

Gordon (1958) proposed a method by which the electron densities and electron and ion temperatures could be determined by analyzing the backscatter power. Further studies of the scattering mechanisms by Fejer (1960), Salpeter (1960a,b), Buneman (1962), and Dougherty and Farley (1960) resulted in the ionospheric radar equation, relating the electron density N to the system parameters.

$$N = \frac{32\pi^2 R^2 P_R}{P_T \sigma \lambda^2 \tau c \overline{G}} \qquad (1.1)$$

where P_T is the transmitted power

P_R is the power returned

R is the range to the scattering volume

λ is the exploring wavelength

τ is the transmitted pulse length

c is the velocity of light in free space

When the magnetic field and collisions can be neglected, the observed electron cross section, σ, is given by Buneman (1962) as

$$\sigma = \sigma_e \left[1 - \frac{1}{1 + (\frac{4\pi D}{\lambda})^2} + \frac{1}{\left[1 + (\frac{4\pi D}{\lambda})^2\right]\left[1 + (\frac{4\pi D}{\lambda})^2 + \frac{T_e}{T_i}\right]} \right] \qquad (1.2)$$

for $T_e/T_i \leq 3$

where σ_e is the electron cross section $= 4\pi r_e^2 = 10^{-28} m^2$

r_e is the classical electron radius

D is the Debye length $= (kT_e/4\pi Ne^2)^{\frac{1}{2}}$

k is the Boltzmann's constant

e is the electron charge 4.803×10^{-10} ESU

T_e is the electron temperature

T_i is the ion temperature

The backscatter gain, $\overline{G}$, is defined as

$$\overline{G} = \frac{1}{4\pi} \int_0^{\theta_m} \int_0^{2\pi} G^2(\theta,\phi) \sin\theta \, d\phi \, d\theta \qquad (1.3)$$

where $G(\theta,\phi)$ is the antenna gain

ϕ is the azimuthal angle measured with respect to a vertical plane containing the beam axis

θ is the polar angle measured from the beam axis

θ_m is the upper bound on the integral over the polar angle determined, in general, by the antenna gain pattern and the altitude variation of the electron density.

It is of interest to determine the accuracy with which the electron density can be measured both absolutely and relatively. Absolute electron densities are obtained by solving Equation (1.1). Relative electron density measurements can be made by noting that Equation (1.1) may be written as

$$N = \frac{K\ P_R\ R^2}{\left[1 - \frac{1}{1 + (\frac{4\pi D}{\lambda})^2} + \frac{1}{\left[1 + (\frac{4\pi D}{\lambda})^2\right]\left[1 + (\frac{4\pi D}{\lambda})^2 + \frac{T_e}{T_i}\right]}\right]} \tag{1.4}$$

where $$K = \frac{32\ \pi^2}{P_T \sigma_e \lambda^2 \tau c \bar{G}} \tag{1.5}$$

Since K is independent of altitude, a relative electron density profile can be obtained from measurements of P_R, R, and the denominator of Equation (1.4). This relative profile can be normalized and if the electron density at any altitude is known, an absolute electron density profile may be calculated.

The accuracy with which these profiles can be obtained is dependent upon the accuracy with which the parameters can be measured. The resolution with which these parameters can be measured is dependent on the equipment used.

It is of interest in this study to determine the accuracy with which those factors affecting the calibration factor K can be determined, to determine the causes of statistical and diurnal or other variations, and to investigate possible methods of minimizing such variations. It is also of interest to investigate methods of improving the accuracy of the relative profiles as these affect the accuracy with which the calibration factor K can be measured and the accuracy of the electron density profile when other independent calibration sources are available.

In applying Equation (1.2) certain simplifying assumptions are made with regard to magnetic field, collisions, and ionospheric composition. The effect of these assumptions on the accuracy of the observed electron cross section must also be considered.

In general, the problem studied in this investigation is the estimate of the errors involved in various calibration procedures and the comparison of these errors with theoretical estimates and with each other.

1.2 Previous Related Studies

1.2.1 Development of the Ionosphere Radar Equation

J. J. Thomson (1906) showed that all charged particles are capable of scattering electromagnetic waves. Free electrons in an ionized medium will under special conditions scatter electromagnetic waves incoherently and the returned power spectrum will be spread in frequency due to a Doppler effect caused by the thermal motion of the electrons. Gordon (1958) proposed that a powerful radar would be capable of detecting the weak backscattered signal and thus such a method could be used to determine the electron density and electron and ion temperatures in the earth's ionosphere. Based on Gordon's proposal, the power returned from a vertically directed pulse radar system is given by

$$P_R = \frac{P_T c \tau \lambda^2 \sigma_N}{32\pi^2 R^2} \bar{G} \tag{1.6}$$

where $\sigma_N = N\sigma_e$, and the remaining parameters are those as defined by Equation (1.1).

Fejer (1960) showed for the case of thermal equilibrium and in the absence of a magnetic field that σ_N is dependent on the exploring wavelength and the Debye length. For $\lambda << 4\pi D$, $\sigma_N = N\sigma_e$, which is the result given by Gordon. In this case the scattering can be thought to be from individual electrons. For $\lambda >> 4\pi D$, $\sigma_N = \frac{N\sigma_e}{2}$. In this case the scattering can be thought to be the result of density fluctuations in the plasma.

Buneman (1962) showed that in the absence of the magnetic field and in the absence of collisions that

$$\sigma = \sigma_e \left[1 - \frac{1}{1 + (\frac{4\pi D}{\lambda})^2} + \frac{1}{\left[1 + (\frac{4\pi D}{\lambda})^2\right] \left[1 + (\frac{4\pi D}{\lambda})^2 + \frac{T_e}{T_i}\right]} \right]$$

$$\text{for } T_e/T_i \leq 3$$

In the derivation it was assumed that m_i/m_e is so large as to be considered infinite.

The spectra of the backscatter signal are very dependent upon ion composition. Studies in this area have been made by Petit (1963), Moorcroft (1964), and Evans (1967).

The effects of neutral collisions on the spectrum are dependent on the magnitude of the exploring wavelength as compared to $4\pi D$. For the case of $\lambda >> 4\pi D$ various investigations have been made. Dougherty and Farley (1963) showed that collisions of ions and electrons with neutral particles are effective below 150km for a probing frequency of 50MHz. At frequencies greater than 50MHz collisional effects are weaker. It was also pointed out that while collisions affect the shape of the spectrum, they have no effect on the total scattered power.

The introduction of the earth's magnetic field will have various effects on the spectra depending on angle between ray and magnetic field and the relative values of ion gyroradius, electron gyroradius, and exploring wavelength. These cases were discussed by Evans (1967).

1.2.2 Backscatter Gain Measurements

Warner (1967) calculated backscatter gains at the Arecibo Ionospheric Observatory from data obtained from N11 type ionospheric experiments. For a series of 13 such experiments covering a period of approximately three years, the calculations showed an average increase in gain of about 3db from day to night. Similar conclusions had been arrived at by Wagner at the Arecibo Ionospheric Observatory and Doupnik at The Pennsylvania State University.

1.2.3 Plasma Line Measurements

The backscatter power returned from the ionosphere is the sum of the power returned from the ionic component and the electron component. The relative distribution of power between these components is dependent on the ratio of the exploring wavelength to $4\pi D$. For typical exploring wavelengths, $\lambda >> 4\pi D$, almost all of the returned power is due to the ionic component. There is, however, an extremely small amount of power which is associated with the electronic component and which appears as a pair of spikes symmetrically displaced from the radar frequency (Salpeter, 1960a; b), (Dougherty and Farley, 1960), (Fejer, 1961). The amount of displacement in the absence of magnetic field is

$$f_e = \pm f_N \left[1 + 3 \left(\frac{4\pi D}{\lambda}\right)^2\right]^{\frac{1}{2}} \qquad (1.7)$$

where f_N is the plasma frequency = $(Ne^2/\pi m_e)^{\frac{1}{2}}$.

The plasma lines are caused by the Doppler shift introduced by scattering from the weakly damped longitudinal electrostatic plasma oscillations with frequency, f_e, wavelength, $\lambda/2$, and phase velocity, $v_{ph} = f_e\lambda/2$. The width of the plasma line is dependent upon electron-ion collisions, Landau damping, transmitter pulse length, and electron density variation with altitude (Perkins and Salpeter, 1965).

Although the electron component backscatter power per unit bandwidth is high, it is not possible to obtain plasma line measurements with existing techniques under nighttime conditions. However, if the plasma line is enhanced by fast photoelectrons moving at the same velocity as the phase velocity of the wave, suitable measurements can be obtained. Fast photoelectrons are present during the day at certain altitudes.

Perkins et al. (1965) made plasma line measurements at the Arecibo Ionospheric Observatory during January, February, and March of 1965. After small corrections for magnetic field and electron temperature effects were made, profiles for electron density were obtained. The values obtained were compatible with the previous measurements at Arecibo from ionosondes and the ion component of ionospheric backscatter.

Yngvesson and Perkins (1966) made a series of plasma line, power profile, and 500μsec spectra measurements at Arecibo in October of 1966. The measurements were made above the F2 peak. A noise source of 50K was used for the calibration of the system. The average backscatter gain defined by equation (1.1) was calculated from data obtained during six runs as $\overline{G} = 43.5 \pm 0.5$db. These results correspond to fall daytime conditions.

1.2.4 Antenna Gain Calibration

Thome (1963) obtained an on zenith antenna gain pattern for the Arecibo dish during the passage of the 3C33 radio source at 17:00 on November 21, 1963. The pattern, as shown in Figure 1, was constructed by averaging the measured values on each side of the maximum. The gain included losses up to the preamplifiers.

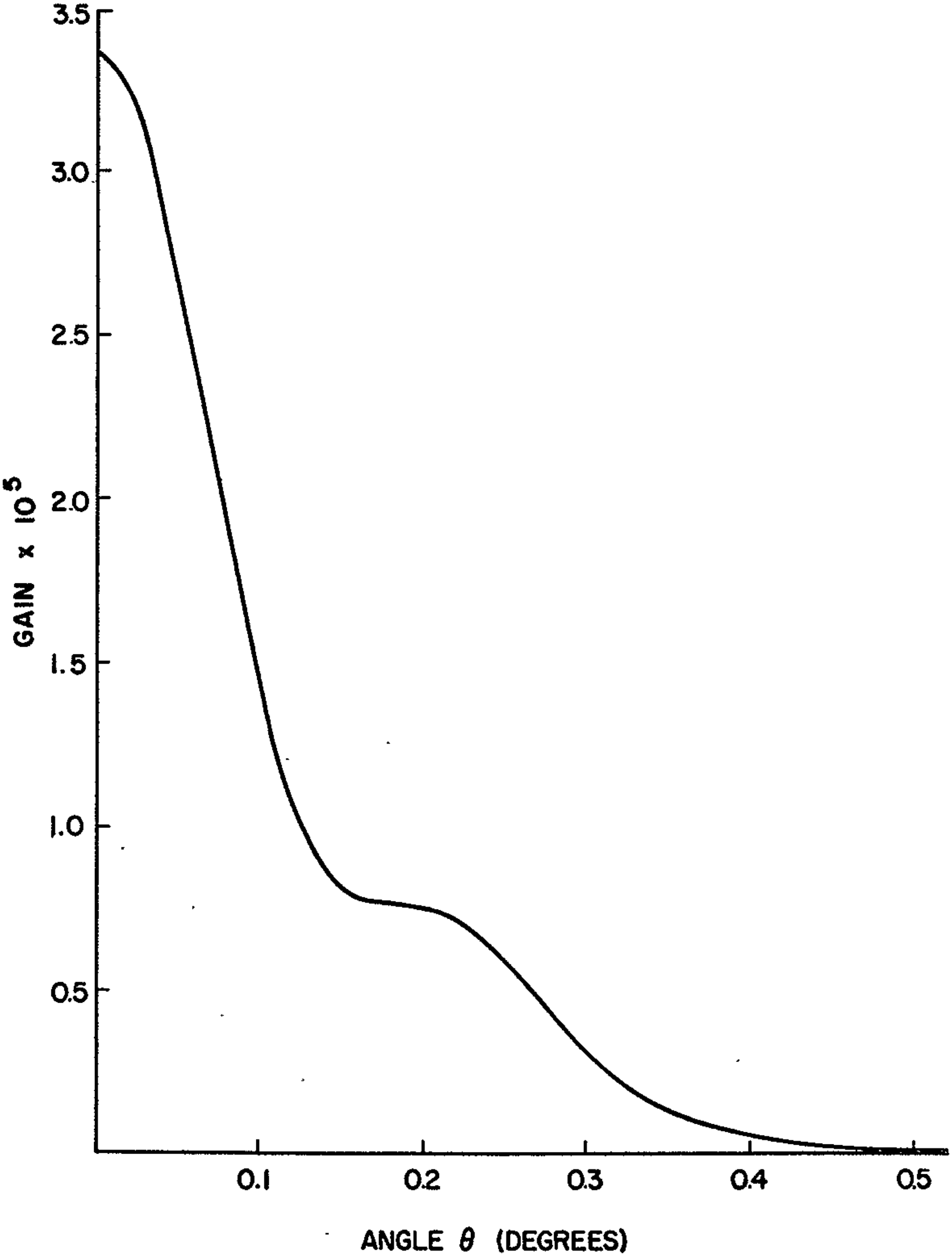

MODEL ANTENNA PATTERN

FIGURE 1

From the pattern the peak antenna gain was found to be 55.25db. If the pattern can be assumed to be azimuthally symmetric and if transmitting losses can be assumed to be equal to receiving losses, the backscatter gain as given by Equation (1.3) reduces to

$$\overline{G} = \frac{1}{2} \int_{0}^{.5^{\circ}} G^{2}(\theta) \sin \theta \, d\theta \qquad (1.8)$$

Using Equation (1.8) and the measured pattern, the backscatter gain was calculated to be 48.5db.

Hardebeck (1965) ran a series of experiments using radio sources to measure the antenna gain for various modes of operation. The fluxes of the sources were known to within .5db. For one experiment both nighttime and daytime measurements were made at various zenith angles. Though no consistent gain change was observed between the daytime and nighttime data, it was observed that the point scatter for the nighttime measurements was less than that for daytime measurements. Most observations were made over a range of zenith angles greater than 4°. However, measurements were made for one daytime source and one nighttime source with zenith angles of 1.19°S and 1.39°S respectively. The magnitude of the gains measured were 55.76db and 56.83db with the higher gain corresponding to the nighttime measurement.

1.2.5 Noise Source Calibration

Hardebeck (1965) made measurements with regard to the noise tube (calibration source). The manufacturer specified the error in the noise source, its attenuators, and directional couplers to be within $\pm$ 1db. With the 10K setting used this would correspond to a range of 8 to 12.5K. The measurements made gave a noise temperature of 12.1K, however, some reservation about these results were expressed by Hardebeck.

An overnight run was made to determine the stability of the noise source. Measurements were made at 30 minute intervals. These tests showed that the variations over the period were of the order of .3db. However, since receiver gain variations and noise source variations could not be separated, these results can be attributed to noise source variation only if the receiver gain variations can be considered negligible.

1.2.6 Study of the Reflector Surface

The Arecibo reflector, a 1000 foot aperture, is a segment of a sphere with a radius of 870 feet. The reflector surface is supported by two orthogonal sets of cables anchored on the perimeter. Ten 1 1/4 inch galvanized bridge strand cables span the reflector from north to south. These are the lower supporting cables. Three hundred and eighteen 3/8 inch bridge strand cables span the reflector from east to west. These are the upper supporting cables. The upper cables are clamped to the lower cables at each intersection. It is the upper cables which support the reflector surface mesh.

Forrest (1965) studied the reflector system with regard to effects of temperature variation on reflector contour. The lower cables showed no noticeable dimensional effects due to temperature changes. The upper cables showed a linear sag of 1.2 mm/^{o}F over the temperature range of 60^{o}F to 90^{o}F at the center of each 100 foot bay as determined by the lower supporting cables. There was no sag at the intersection of the upper and lower supporting cables.

Forrest photogrammetrically measured the standard deviation of the reflector surface from the design value of 870 feet. At 76^{o}F the raw standard deviation was $\pm$.110 feet. This value was reduced to $\pm$.085 feet at 60^{o}F, the optimum operating temperature. The 60^{o}F optimum temperature is determined by the upper cable sag being adjusted to its nominal value at this temperature.

Philipson (1968) photogrammetrically calibrated the Arecibo Ionospheric Observatory reflector from the center structure. This method is basically the same as used by Forrest in the earlier calibration except that the accuracy requirements were more stringent for the 1968 calibration. From observations made at 92^{o}F Philipson calculated the optimum reflector radius to be 869.861 feet and a standard error of $\pm$0.14 feet. Using Forrest's center span upper cable movement gradient of 1.2 mm/^{o}F, Philipson calculated optimum radii for various average temperatures. These are shown in the following table.

Table I

Reflector Surface Temperature Study

Average Cable Temperature (°F)	Optimum Reflector Radius (ft.)	Standard Error of a Single Observation (ft.)
60	869.976	±.110
70	869.941	±.118
80	869.905	±.128
92	869.861	±.141

The overall accuracy of the calibration was estimated to be 11 mm.

1.2.7 Accuracy of the Electron to Ion Temperature Ratio

Perkins and Wand (1965) compared two ways of determining the electron to ion temperature ratio by digital methods at Arecibo. Ratios were measured from the autocorrelation functions and power spectra of the returned signals. The autocorrelation functions were obtained by forming lagged products from samples of data measured at 20μsec intervals. The power spectra were obtained by Fourier transforming the autocorrelation functions.

Electron to ion temperature ratios were determined from the autocorrelation functions by comparing the time of the first crossing and depth of the first minimum with a set of theoretical values relating these parameters to the electron to ion temperature ratio. This ratio was determined from the power spectrum by comparing the wing to center ratio and half power bandwidth with a set of theoretical values. In each case the theoretical curves were calculated by assuming that only O^+ ions were present in the region under study.

In general, the values of the electron to ion temperature ratios determined by the two methods agreed within 10 percent for signal to noise ratios greater than unity. It was suggested by the authors that more reliable electron to ion temperature ratio data be obtained by performing a least square fit of experimental spectra with theoretical spectra.

1.3 Specific Statement of the Problem

The problems to be considered in this study are as follows:

1. What is the backscatter gain required in Equation (1.1) to relate the received power to the electron density? What is the variation in this backscatter gain with time and other parameters and what is the predominant effect causing such variations?
2. What is the accuracy with which each of the basic parameters in Equation (1.1) can be determined? What effect does each have on the accuracy of the measurement of the electron density?
3. How do different methods of measuring the backscatter gain agree? Which method is most suitable for measuring the backscatter gain or normalizing the profile under given circumstances?

4. What methods can be used to reduce the diurnal variation in the system calibration factor and what system changes could reduce these fluctuations?

CHAPTER II

EXPERIMENTAL DETAILS

2.1 Description of Equipment Used for Incoherent Backscatter Measurements

At the Arecibo Ionospheric Observatory a 40MHz transmitter and a 430MHz transmitter are available for ionospheric studies. For the present study only the 430MHz transmitter was utilized. This transmitter is capable of producing 2.5MW peak power at a maximum duty cycle of six percent. The pulsing of the transmitter is controlled from the receiver room.

Power from the transmitter is sent to the line feed through 1400 feet of WR-2100 waveguide. Measurements of power transmitted are made at the transmitter side of the waveguide and indications are given by means of a bolometer, connected to a directional coupler and located in the transmitter room. A motor driven E-H tuner, which is controlled in the transmitter room, is used to match the transmitter to the waveguide.

At the line feed side of the waveguide, the signal is fed through a high power duplexer and into one arm of the cross shaped turnstile. Two of the arms of the turnstile contain sliding plungers which are used to excite different beam polarizations (linear or circular either sense). The fourth arm feeds a low power duplexer. There is approximately 23db of isolation between the lower power arm and high power arm of the turnstile.

The turnstile junction drives the line feed which is a 96 foot long section of square, tapered, slotted waveguide. The design amplitude distribution of the line feed was to approximate a tapered Gaussian distribution across the aperture, but the design criteria were not realized.

Figure 2 shows the receiver system used for the majority of tests discussed in this report. The receiver section can be connected to two possible inputs, the high power arm or the lower power arm of the turnstile. Ionospheric experiments use the low power input. Initially, the signal is fed through a 10db or 20db directional coupler through which the calibration noise pulse is introduced. In the experiments prior to December 1968 it was then fed through an electron beam parametric amplifier to a power splitter and next to close range receivers one or two (CRR1 or CRR2). CRR1 and CRR2 each contain a preamplifier, mixer, and an intermediate frequency amplifier. The difference between the two configurations is that CRR1's local oscillator is fixed, whereas the oscillator in CRR2 is variable. For the December 1968 experiments a new duplexer, which eliminated the need for the protecting features of the electron beam parametric amplifier, was available, and hence, a lower noise solid state front end was able to be employed.

The 30MHz intermediate frequency from the carriage house is transmitted to the receiver room through 1400 feet of RG-17u coaxial cable. In the receiver room the usual

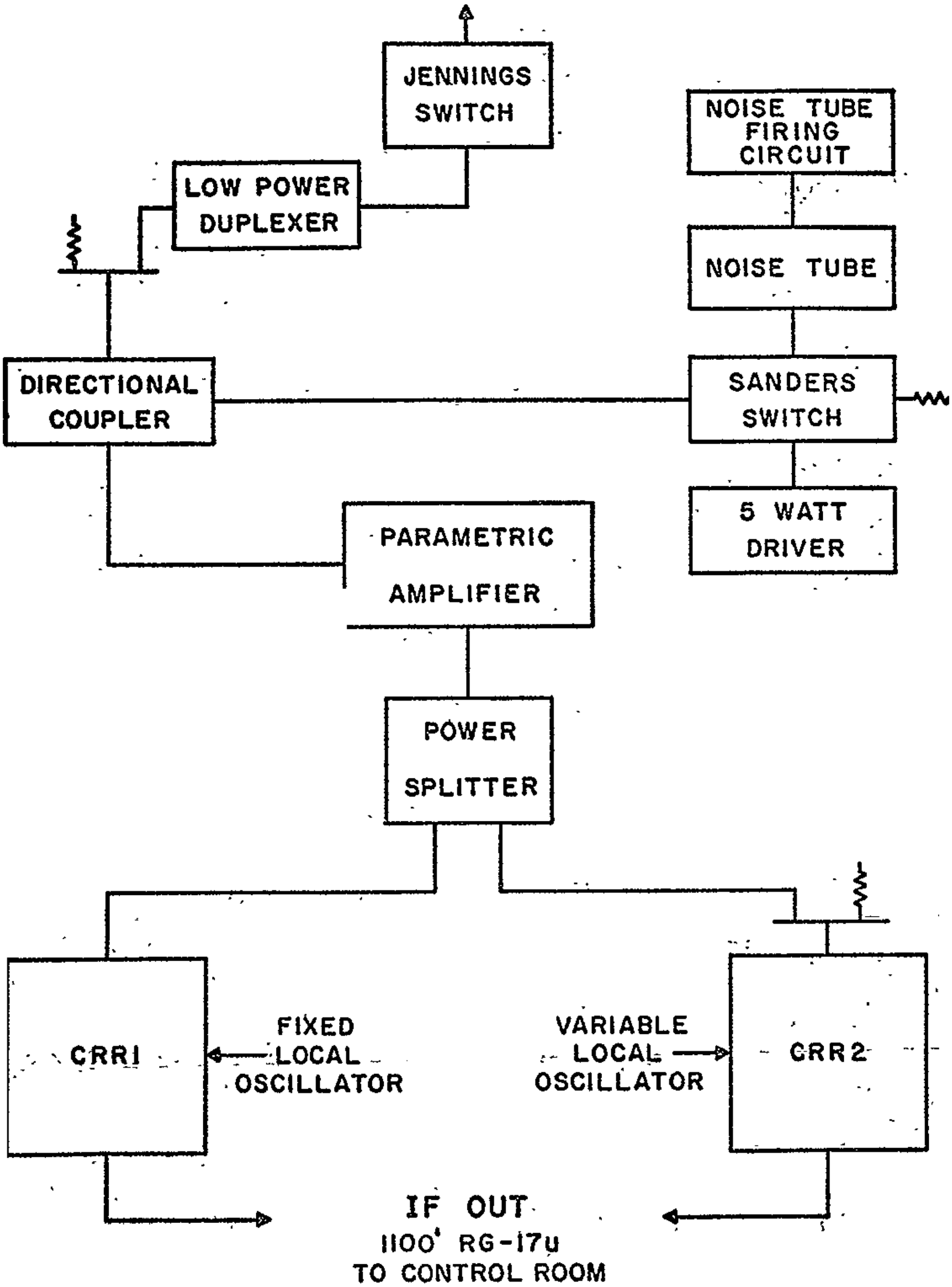

APPARATUS IN CARRIAGE HOUSE
FIGURE 2

equipment configuration for the ionospheric experiments under study is shown in Figure 3. It should be noted that each channel contains an attenuator. The purpose of the attenuator is to control the input to the analog to digital converters.

A digital computer controls the sampling at the analog to digital converters.

2.2 Description of Incoherent Backscatter Measurements

2.2.1 Measurement of the Power Profile

For ionospheric studies it is required to measure the amplitude and the autocorrelation function or frequency spectrum of the backscatter signal as a function of altitude. To do this data is recorded from three channels: the density channel, the recovery channel, and the autocorrelation channel. A block diagram of this sytem is shown in Figure 3.

The density profile is obtained by taking samples of the center frequency signal, which is bandlimited by a filter large enough to include the sidebands due to the ionic component of the backscatter power and mixed to an intermediate frequency of 100KHz, at intervals which are usually set to 20μs. Because the transmit-receive tube and and perhaps other parts of the system introduce noise which is enhanced during the period just after the transmitted pulse and during the time observations are being made, a second channel, the recovery channel, has been introduced.

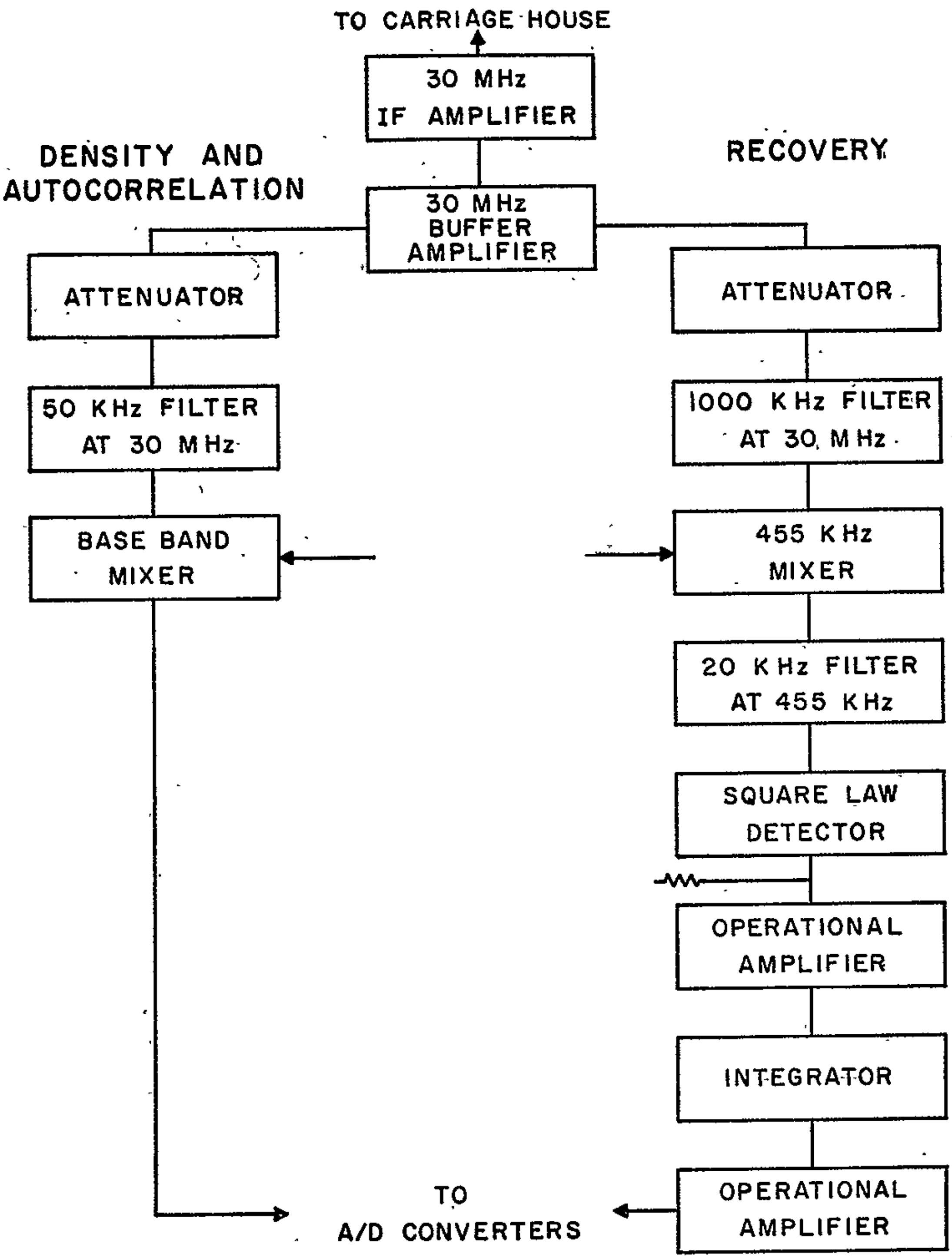

APPARATUS IN CONTROL ROOM

FIGURE 3

For this channel the local oscillator in the receiver room is adjusted to offset the sampling 355KHz from the center frequency. This results in a noise behavior that is similar to the density channel but without the ionospheric signal. This channel is used to compensate for noise effects in the density channel.

Receiver and system gains may vary. To ensure that absolute power measurements can be made, a noise pulse is introduced into the system during each interpulse period at an altitude sufficiently great that the ionospheric backscatter return is negligible.

2.2.2 Measurement of the Electron and Ion Temperatures

The autocorrelation channel is used to obtain autocorrelation functions of the backscatter signal spectra. The autocorrelation functions are formed from lagged products of data taken at specified intervals. For N11 type experiments the sampling interval is 20μs and 25 samples are obtained which have correlation with each other. The lagged products are formed by either of the following schemes.

$$M_R(\ell\Delta t) = \sum_{n=-12}^{12-\ell} S_{n+\ell}S_n \tag{2.1}$$

$$M_S(\ell\Delta t) = \begin{cases} \sum S_{-\frac{\ell}{2}} S_{\frac{\ell}{2}} & \ell \text{ even} \\ \sum S_{-\frac{1}{2}(\ell-1)} S_{\frac{1}{2}(\ell+1)} & \ell \text{ odd} \end{cases} \tag{2.2}$$

where S_i is the sampled signal and

$$-12 \leq i \leq 12$$

$$0 \leq \ell \leq 24$$

The mean lagged products are obtained by averaging the above expressions over a large number of radar pulses. For the N12 experiments the lagged products are formed from four different pulse configurations in order to produce an autocorrelation function with improved height resolution.

By comparing the measured autocorrelation functions with theoretical values electron to ion temperature ratios and ion temperature ratios can be determined. This is done by forming least square fits, using the time of the first crossing and depth of the first minimum, or Fourier transforming the autocorrelation function to the frequency spectrum from which the half power bandwidth and wing to center ratio can be obtained. The N12 analysis program employs the first two methods while the N11 analysis program uses the last two.

2.3 Simplifying Assumptions to the Ionosphere Radar Equation

In applying the ionospheric radar equation, (1.1), to ionospheric studies, certain simplifying assumptions in the observed electron cross section term are sometimes made to facilitate the making of measurements and calculations. These assumptions are usually dependent upon the site of the experiment and the altitude range under study.

The expression for the observed electron cross section as given by Equation (1.2) neglects the effects of the magnetic field and collisions and is valid for electron to ion temperature ratios equal or less than three.

The error caused by neglecting the magnetic field can be observed from Figure 4. This curve was constructed for the magnetic field effects at Arecibo using theoretical curves from Farley (1966). For electron to ion temperature ratios of unity no error is present, but as the electron to ion temperature ratio is increased the error becomes prominent. The error is one which underestimates the true value for the observed electron cross section. For the present study corrections were made for the error introduced by neglecting the magnetic field. These corrections never exceeded 2.1 percent.

Figure 5 (Dougherty and Farley, 1963) shows the effect that collisions have on the ionic component of the back-scatter power. It should be noted that the total scattered power is independent of the collision frequency, but that the shape of the spectrum is altered. It can be seen that above 160km the error in the shape of the spectrum due to neglecting collisions is less than .1 percent.

After the conditions of using Equation (1.2) have been justified, it still remains necessary to calculate a value for the observed electron cross section. To do this it is necessary to know the electron to ion temperature ratio and $(4\pi D/\lambda)^2$. The methods of determining the electron to ion

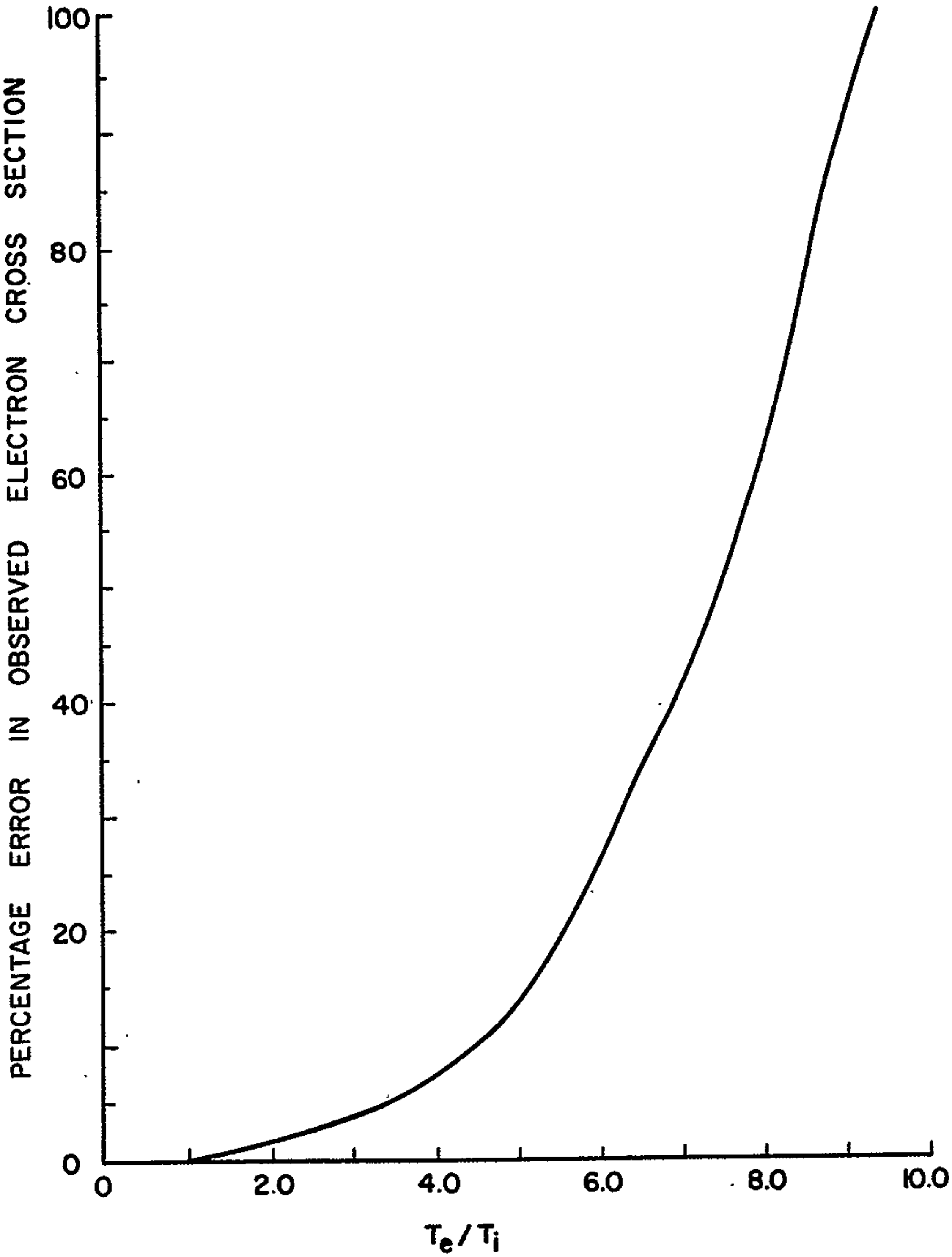

ERROR CAUSED BY NEGLECTING MAGNETIC FIELD

FIGURE 4

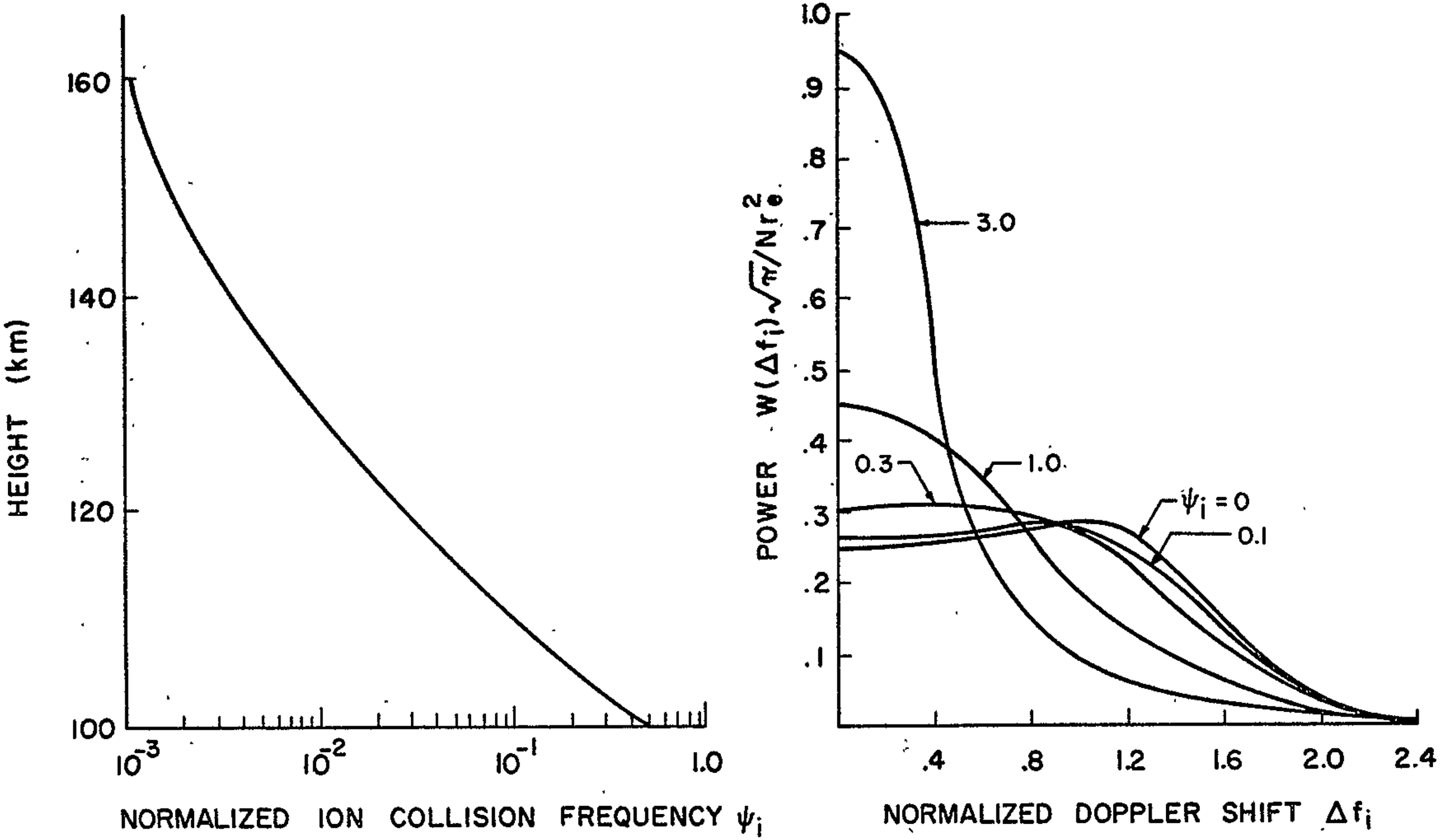

EFFECT OF COLLISIONS ON THE IONIC COMPONENT (DOUGHERTY AND FARLEY 1963)

FIGURE 5

temperature ratios as discussed in section 2.2.2 involve the comparison of measured autocorrelation function or power spectra with theoretical ones.

The autocorrelation functions or their spectra are dependent on ion composition. Though this poses no problem in comparing measured with theoretical autocorrelation functions or spectra when a single ion is present, unique comparisons are quite difficult when mixtures of ions appear. For the case of mixtures, assumptions must be made to determine the electron to ion temperature ratio. In general, the analysis programs for determining the electron to ion temperature ratio assume that oxygen ions predominate in the region of the F2 peak. In this study the validity of this assumption was checked using a models program developed by Nisbet (1970) and proper compensation was made when necessary.

The analysis programs used in the present study employed the equation

$$N = \frac{KP_R R^2}{1 + \frac{T_e}{T_i}} \qquad (2.3)$$

to obtain electron density profiles. This equation is obtained from Equation (1.4) by assuming that the term $(4\pi D/\lambda)^2$ is zero. It was necessary to account for the errors introduced by making this assumption when they were significant.

2.4 Description of N11 and N12 Experiments Used for the Present Study

For the N11 and N12 ionospheric experiments in the present study the received equipment configuration was the same and is shown in Figure 3. The chief difference lay in the manner in which the pulses were transmitted and the way in which the backscatter signal was sampled and analyzed. For the N11 experiments 40μs and 500μs pulse were transmitted alternately over ten and fifteen minute periods respectively. Density and recovery channel data were obtained for each type of pulse. Autocorrelation channel data were obtained from the 500μs pulses and from these electron to ion temperature ratios were obtained at 75km increments by methods described in section 2.2.2. It was assumed that only oxygen ions predominated.

The N11 analysis program was used to produce combined corrected profiles by using 40μs power profile up to 400km at which point it was joined to the 500μs power profile. The combined profiles were corrected for electron to ion temperature ratio differences by use of Equation (2.3). Between the altitudes of 250km and 475km, the combined power profiles were corrected by using the values of the electron to ion temperature ratios as determined from the 500μs data. Above and below this altitude range electron to ion temperature ratios, obtained by assuming that the electron to ion temperature ratios were equal to one at 1000km and 100km and then by interpolating between these values and those at 475km and 250km respectively, were used to correct the profile.

The N12 experiment stepped the transmitter to produce a series of four different pulse configuration. These were

1. a single 100μsec pulse
2. a single 160μsec pulse
3. two 100μsec pulses with 160μsec spacing between pulses
4. two 100μsec pulses with 300μsec spacing between pulses

The usual interpulse period for each configuration was 9.3msec. Each configuration was run 500 times and after ten such cycles a block of data was recorded.

Density and recovery channel data were obtained from the single 100μsec pulse configuration only. Autocorrelation channel data were obtained from all four pulse configurations using different delays with different configurations. Electron to ion temperature ratios were obtained from the autocorrelation channel data by assuming oxygen ions in the region between 250km and 430km and using the method described in section 2.2.2. The electron to ion temperature ratios above 430km were assumed to be equal to the 430km value. Below 250km the temperature ratios were obtained from temperature models when they existed and then by interpolating down to an assumed ratio of one at 100km. Using these electron to ion temperature ratios, the power profile was corrected by employing Equation (2.3).

2.5 Procedure

For the calibration study, data were obtained at the Arecibo Ionospheric Observatory for three N11 experiments and seven N12 ionospheric experiments. The N11 data were taken during December of 1967. Data for the N12 experiments were taken during the summer of 1968, December of 1968, and the summer of 1969. Gain calculations and analysis were made using this data.

Additional experiments were performed during the summer of 1968 to check receiver linearity, attenuation setting effects, reflected power effects, and reflector surface temperature effects. During the December of 1968 experiments, measurements were made to determine what effects waveguide losses might have on the gain. In the summer of 1969, a thermocouple was installed on a cable near the support platform in order to study feed displacement effects.

CHAPTER III

EXPERIMENTS, RESULTS, AND ANALYSIS

3.1 Effect of Reflections Due to Transmitter-Waveguide Mismatch

During the N11 and N12 ionospheric experiments the waveguide incident power and the waveguide reflected power are monitored at periods of approximately 30 minutes. Under normal operating procedures, the waveguide is retuned if the reflected power is greater than 4 percent of the incident power.

To determine the effect an abnormal amount of reflected power might have on the measured parameters, the waveguide was detuned during the N12-44 experiment to produce a reflected power of approximately 8 percent of the total transmitted power. This was done for a run of 6.5 minutes. Data from this run were compared with data from the preceding and succeeding runs. No noticeable effect on any of the measured or calculated parameters, except for the total transmitted power, was observed. The measured total transmitted power decreased by about 4 percent.

It was concluded that providing the transmitted power is measured at the beginning and end of each run, normal operating procedures should ensure that any errors due to line mismatch are negligible.

3.2 Temperature Effect on Waveguide Losses

Theoretically, the losses in a waveguide due to lossy dielectric and finite wall conductivity are given for the TE_{10} mode by

$$\alpha = \frac{\sigma_d}{2\omega} \sqrt{\frac{\mu_d}{\epsilon_d}} \left(\omega^2 - \omega_c^2\right) + \frac{\left(1 + \frac{2b\omega_c^2}{a\omega^2}\right)}{b\ \eta_r\ K} \frac{\mu_m \omega}{2\sigma_m} \text{ nepers/m} \qquad (3.1)$$

where $K = \sqrt{1 - \left(\frac{\omega_c}{\omega}\right)^2}$

$\omega_c = \frac{\pi}{a\sqrt{\mu\epsilon}}$

$\eta = \sqrt{\frac{\mu}{\epsilon}}$

ϵ is the dielectric constant

μ is the permeability

σ is the conductivity

ω is the transmitted frequency

a is the long waveguide dimension

b is the short waveguide dimension

d, m, and v are subscripts which refer to dielect, metal, and vacuum respectively

The transmission system at the Arecibo Ionospheric Observatory uses WR-2100 waveguide and waveguide components. The inside dimensions of this waveguide are .266m by .534m in cross-section. The aluminum walls of the waveguide are .00475m thick. The waveguide is charged with dry air under a pressure of three ounces to prevent condensation and the accumulation of water.

Assuming that the conductivity of the air in the waveguide is less than 10^{-7} mho/m, the attenuation due to the dielectric loss is negligible.

Wall losses were calculated to be approximately .5db with a 50^{o}F temperature change causing a variation of less than .04db.

During the N12-54 experiment the output power of the waveguide was monitored. These measurements were made on a relative basis, hence no information concerning the overall attenuation of the waveguide was obtained. However, changes in the attenuation were calculated. Over a temperature range of 58^{o}F to 83^{o}F and a time interval of 25 hours, the maximum change of attenuation was .3db. The changes were random, showing no correlation with either temperature or time, and were of the same order as the resolution of the oscilloscope used to measure the carriage house power.

It was concluded that the major source of variation was the resolution of the measuring system and that any changes in attenuation correlated with temperature would not exceed .3db over the temperature range from 58^{o}F to 83^{o}F The theoretical values substantiate the conclusions as reached by experiment in that variation in attenuation with respect to temperature variations is not an important factor in controlling the system gain.

3.3 Statistical Errors in the Analog to Digital Converters

Because the analog to digital converter, which is used to sample the ionospheric backscatter signal, has a finite range and a finite number of quantization levels, and since it is possible to take only a finite number of data samples, error is introduced into the digitized data. The extent of the error is dependent upon the input signal to the analog to digital converter. For this study the input signal was assumed to be a continuous random voltage with standard deviation σ, relative average power σ^2, and probability distribution

$$p(v) = \frac{1}{\sigma\sqrt{2\pi}} \exp\left(-\frac{v^2}{2\sigma^2}\right) \qquad (3.2)$$

where v is the voltage of the signal.

At Arecibo the analog to digital converter has an input range from -2.5v to +2.5v and an output of 254 quantization levels whose assigned values are $\pm 1, \pm 3, \ldots\ldots$ ± 253. (The values where assigned in this way to make the quantized output proportional to the center of each quantization range). Thus, the average relative output power is given by

$$\overline{\ell^2} = \sum_{\ell = -127}^{127} (2\ell-1)^2 p(\ell) \qquad (3.3)$$

where $p(\ell)$ is the probability that the signal falls within the ℓth quantization level. The fractional error, α, in output for a given input is defined as

$$\alpha = \frac{\overline{\ell^2} - 4\sigma^2}{4\sigma^2} \qquad (3.4)$$

The factor four, which multiplies σ^2, results from the manner in which the values of the quanitzation levels were assigned.

In order to include the effects of dc levels, which result from drifts in the equipment, equation (3.2) was modified to

$$p(v) = \frac{1}{\sigma\sqrt{2\pi}} \exp\left(-\frac{(v-\mu)^2}{2\sigma^2}\right) \qquad (3.5)$$

where μ is the dc level in bits

one bit is equal to .0197 volts

Using Equation (3.3), (3.4), and (3.5) the fractional error, α, was calculated as a function of relative input power for three dc levels. The results of these calculations are shown in Figure 6. From this figure it can be seen that if the dc level is kept between ± 1 bit, and the input power is kept between 50 bits^2 and 2000 bits^2, errors in the output will be less than one percent. This range is sufficient for typical ionospheric backscatter signals.

In addition to error introduced by the analog to digital converter, an error also results because only a finite number of samples are taken. The signal which is sampled is assumed as before to be Gaussian with zero-mean and standard deviation σ. Since the power in the signal is proportional to σ^2, the sampled data is squared then averaged. Thus, the distribution function of the squared averaged data is

$$W = \sum_{i=1}^{n} \frac{x_i^2}{n} \qquad (3.6)$$

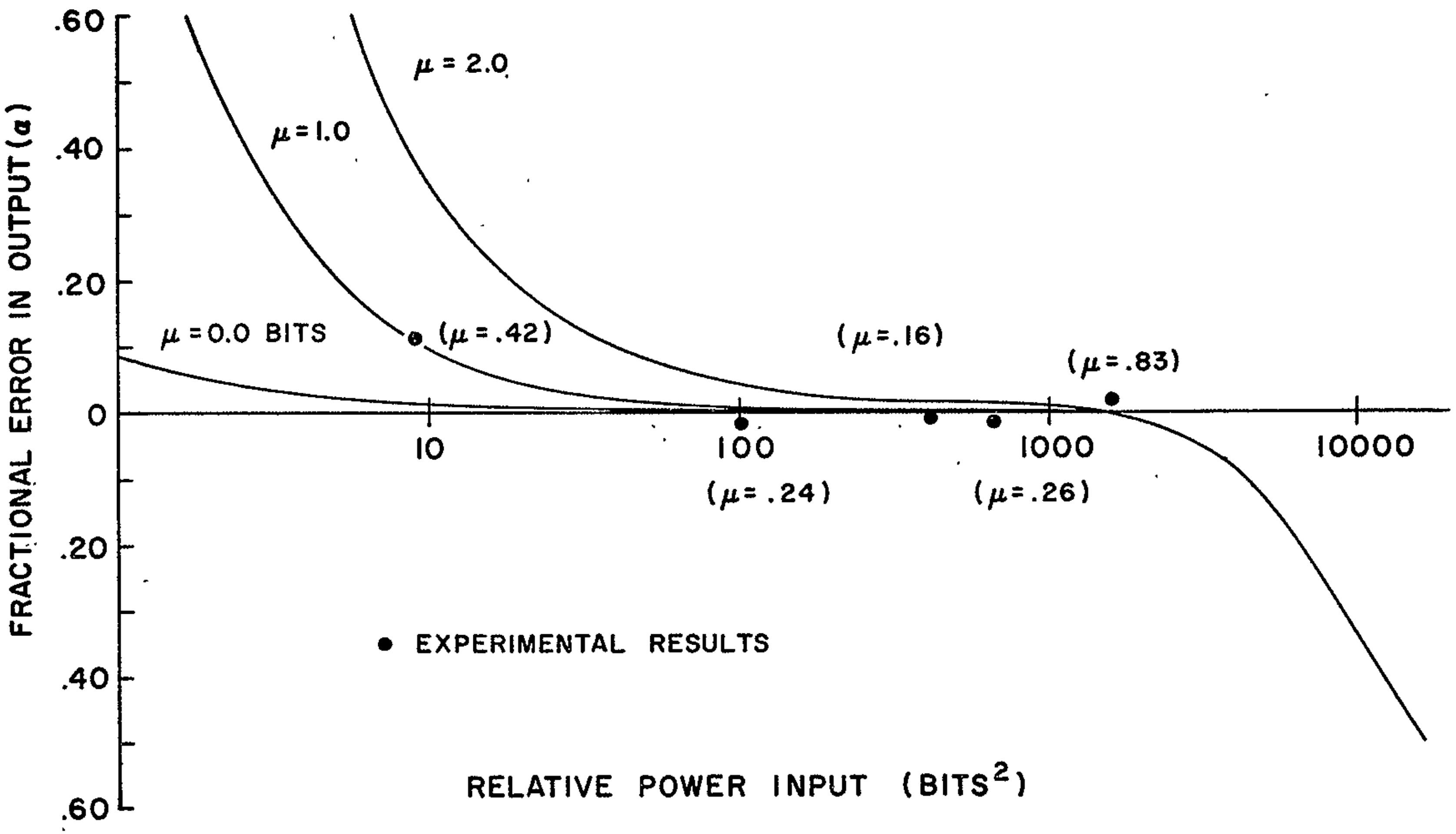

ANALOG TO DIGITAL CONVERTER ERROR

FIGURE 6

where x_i is a random sample from the Gaussian distributed signal input and n is the number of samples.

The distribution function W is a gamma function of n degrees of freedom with a mean equal to σ^2 and a standard deviation equal to $\pm\sqrt{2/n}\ \sigma^2$. For a gamma function with n degrees of freedom the probability of a sample lying within plus or minus one standard deviation of the mean is greater than 68 percent. The probability of the sample lying within plus or minus two standard deviations from the mean is greater than 95 percent. Thus, the error in determining the input power, σ^2, from n data samples is $\sqrt{2/n}$ and $2\sqrt{2/n}$ for confidence levels of 68 percent and 95 percent respectively.

To check experimentally the results given in Figure 6, the levels to the analog to digital converters were varied over a range from 10 bits^2 to 1600 bits^2. For each of the five input levels 425,000 samples were taken so as to keep finite sampling errors less than .8 percent. The fractional errors for each input is given in Figure 6. Corresponding dc levels are shown in parenthesis. The experimental results are seen to agree rather well with the theoretical calculations. The slight deviations are probably the result of statistical errors.

3.4 Receiver Linearity

The individual pieces of equipment that make up the receiver system at the Arecibo Ionospheric Observatory are tested periodically for linearity with regard to output power being proportional to input power. In this experiment the system, as a whole, was tested for this type of linearity. The receiver equipment was set up as for a normal N11 or N12 ionospheric experiment, except that a noise generator was connected to the system at the input to the directional coupler. The noise temperature was varied over a range from 0 to 12,000 K.. Measurements were made for five minutes at each noise generator setting. During the time 200,000 samples of the input were taken squared and averaged by the computer. The relative power output was obtained from the computer print out.of the density channel. This procedure was carried out for two different attenuator settings of the density channel receiver equipment.

The density channel output versus noise meter readings for each attenuator setting are plotted in Figure 7. For the case of 0db attenuation measurements were made for eight different noise input settings. A best fit straight line was obtained using data from the first six points. The last two points were ignored in the curve fitting because of unequal weighting factors. The results are that deviations of the experimental data from the fitted straight line are at most 5.5 percent for any of the eight points.

For the case of 1db attenuation, only four experimental points were measured. Because of unequal weighting factors

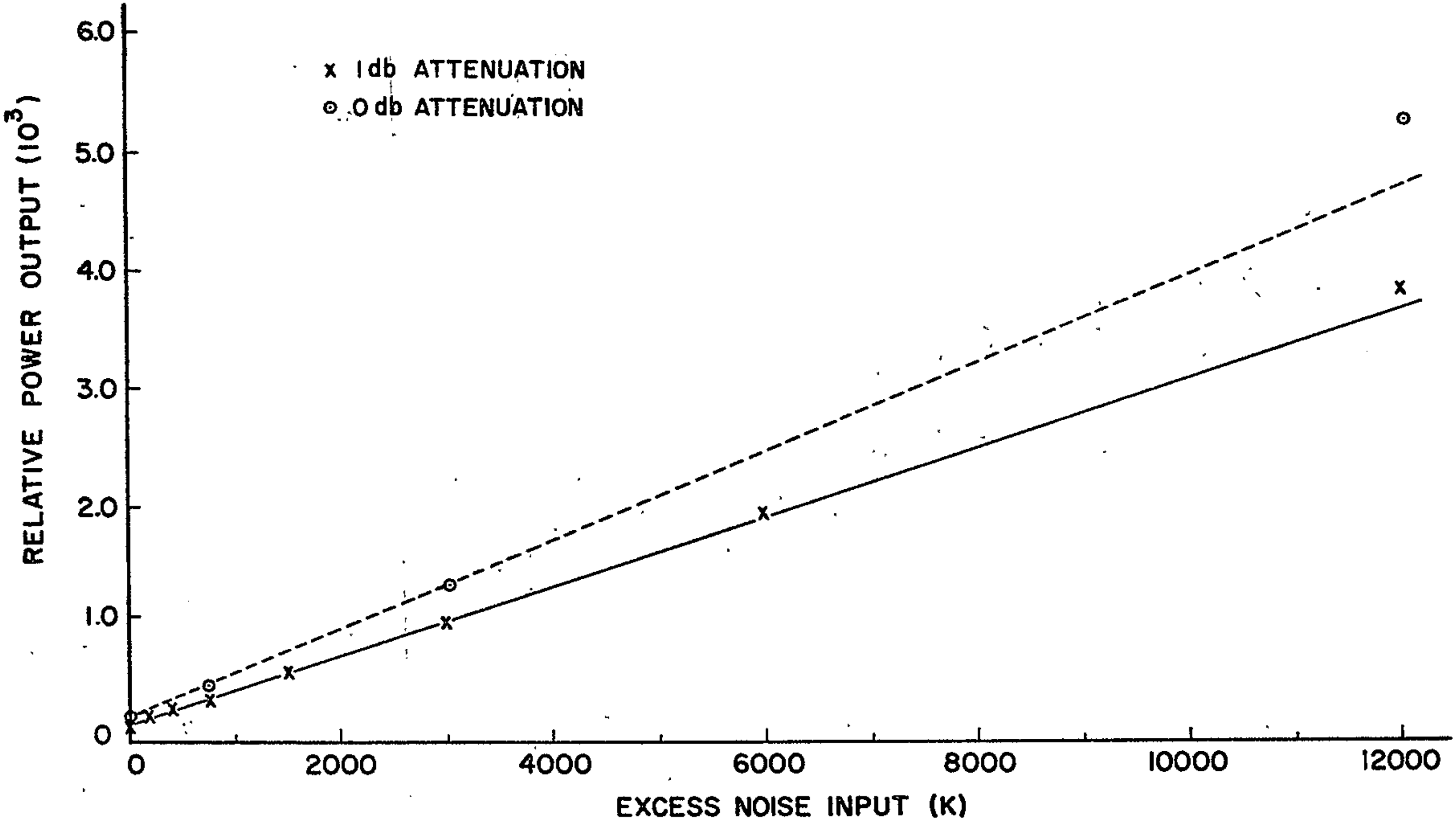

RECEIVER LINEARITY

FIGURE 7

the last point was ignored and a straight line was fitted through the first three points. The last point deviates from this line by 10 percent.

It should be pointed out that the accuracy with which the measurements in this experiment were made is dependent upon:

1. the accuracy of the noise source
2. the number of samples
3. the errors introduced by the finite analog to digital converter

The accuracy of the noise source used as the input signal is probably at best ±5 percent. The error introduced by finite sampling is ±.6 percent. This figure is given with a confidence of 95 percent. Errors introduced by the analog to digital converters are dependent upon the input signal level. Using the results given in Figure 6 of section 3.3, these errors were found to be less than 1 percent for each of the measured data points.

Upon considering the above errors and especially the errors of the noise source, it can only be said that the measured deviations of the data points from the straight line fit are within the accuracies of the equipment and instrumentation used to make the measurements.

3.5 Measured Accuracy of the Observed Electron Cross Section, Height of the F2 Peak, Electron Density, and Power Returned in the Region of the F2 Peak

To obtain a value for the accuracy of data which does not describe any simple geometrical curve, a method of running means was employed. This method assumes that the data be in close time proximity, but does not require any pre-curve knowledge. To obtain the running mean at a certain time, the data point at that time is averaged with the two preceeding and two following points. The variation is the difference between the calculated mean and the center point. The calculated running mean curve is a smooth version of the original curve. If it can be assumed that the measured data vary randomly about the smooth curve, the variation is an indication of the accuracy of the data.

Using this running mean technique the average error in the observed electron cross section was found to be within ±4 percent. This value held for both N11 and N12 type experiments.

Using the same technique the average error in the peak electron density was estimated to be within ±3.5 percent. These calculations were made for runs for which good ionograms existed.

Variations in the heights of the peak were found to be within ±3 percent. This result was obtained using data from the N11-90 experiment and the three summer of 1968 N12 experiments.

The power returned showed variations of ±8 percent in the area of the F2 peak. Included in this number are the effects of calibration pulse variability which are approximately ±3.5 percent (see section 3.9.1).

It should be observed that this technique of obtaining variations in measured parameters includes the real variations of the quantity itself and is thereby an upper limit.

Theoretically, the accuracy of the observed electron cross section, power returned, and height of the F2 peak are dependent upon the signal to noise ratio and the number of samples. For worst case signal to noise ratios at the F2 peak and for the number of samples taken during normal ionospheric experiments, the theoretical accuracies for the power returned and height of the F2 peak are ±4 percent and ±3 percent respectively. Theoretical estimates of the errors in determining the observed electron cross section were made by Perkins and Wand (1965) and were said to be within 10 percent.

3.6 Variation of Peak Antenna Gain

In order to determine the effects of temperatures on the peak antenna gain, an experiment using radio sources was performed by Dr. John Sutton. The method employs a drift scan technique to more accurately pin point the source, after which the antenna is fixed in order to let the source drift through. Sixteen radio sources, whose fluxes are well known, were observed over a period from 04:00 to 10:30. A noise source of known temeperature was used to calibrate the system and the data was recorded on four chart recording channels. Since all of the observations were made off axis, a calibration curve established by Dr. David Jauncey was employed to obtain the on axis gain. From the measurements obtained, the relative peak gain was calculated using the following formula

$$G_p = \frac{PT}{NZØ} \qquad (3.7)$$

where P is the relative power received

N is the relative noise source power

T is the calibration temperature

Z is the zenith angle correction factor

Ø is the flux density of the source

While the gain measurements were being made, the temperatures of three of the upper reflector mesh supporting cables located approximately at the bottom, middle, and top of the bowl, as well as the ambient temperature in the bowl, were recorded. The temperatures were measured by means of thermocouples and the recordings were made on Foxboro model ERB electronic strip chart recorders.

The variation in the calculated gains was random with an average variation of approximately $\pm .5$db and showed no correlation with either time or temperature changes.

3.7 Temperature Measurements

In order to determine whether or not any correlation existed between temperature variations and backscatter gain, during the summer of 1968, thermocouples were installed on three of the upper supporting cables of the reflector surface at approximately the center, middle, and top of the bowl. The thermocouples were placed on the under side of the cables to prevent their coming in contact with the direct rays of the sun. The temperatures were recorded continuously by means of a Foxboro strip chart recorder. After the installation of the thermocouples, the temperatures were recorded during subsequent N12 ionospheric experiments. The diurnal temperatures measured during four N12 experiments are shown in Figure 8.

From the figure it can be seen that diurnal reflector cable temperature variations of at least 20°F are typical at the Arecibo Ionospheric Observatory. The diurnal temperature variation of only 7°F during the N12-52 experiment is an exception to the rule.

Because the temperature measurements of 1968 showed good correlation with respect to backscatter gain variations, measurements were made during the summer of 1969 with an additional thermocouple located on the triangular platform supporting the line feed. The results of these measurements for two ionospheric experiments are shown in Figure 9. From this figure it can be seen that the platform temperature variation differs slightly from the reflector cable temperature variation as a function of time and is generally of a higher temperature.

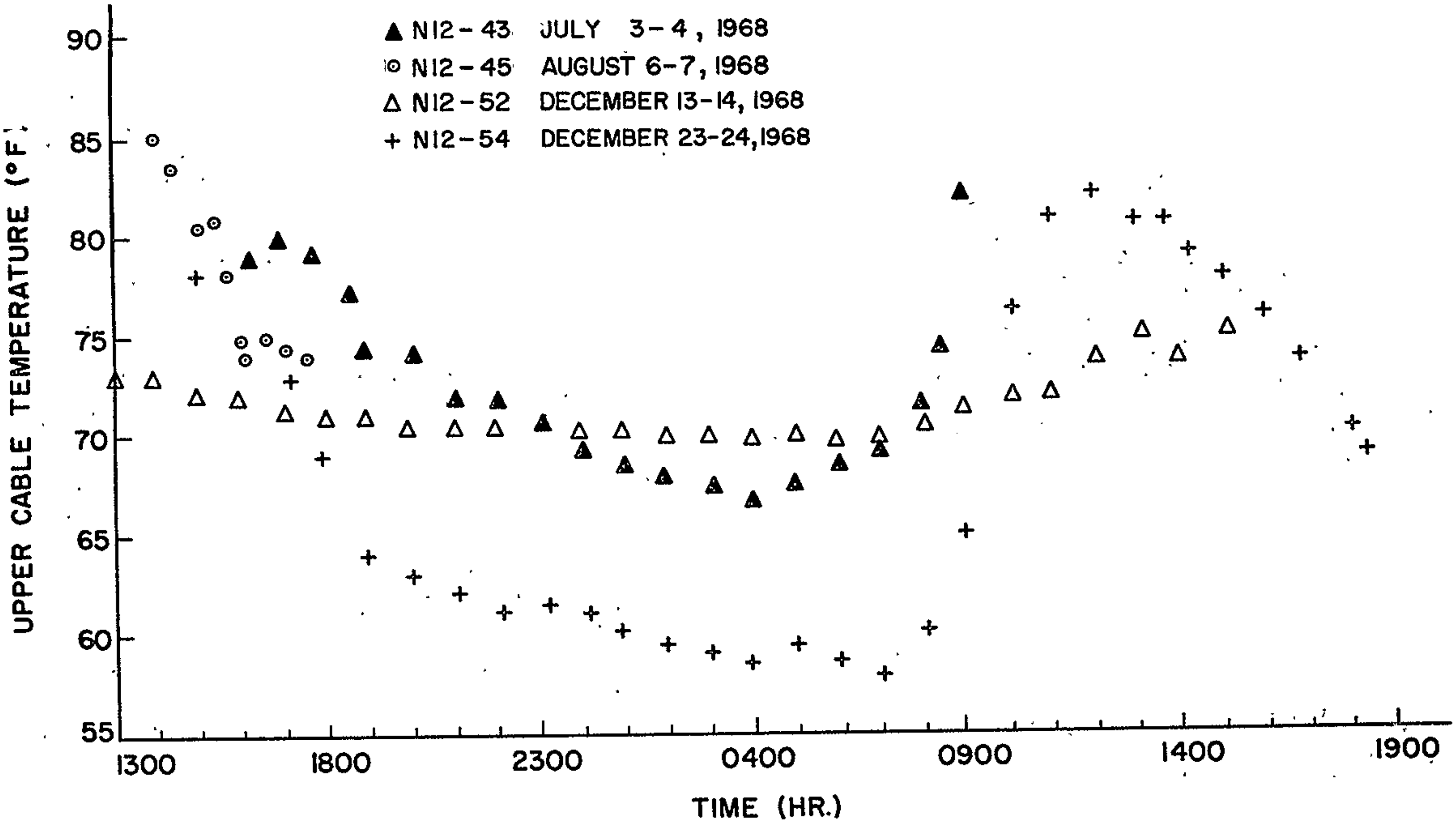

REFLECTOR CABLE TEMPERATURE MEASUREMENTS

FIGURE 8

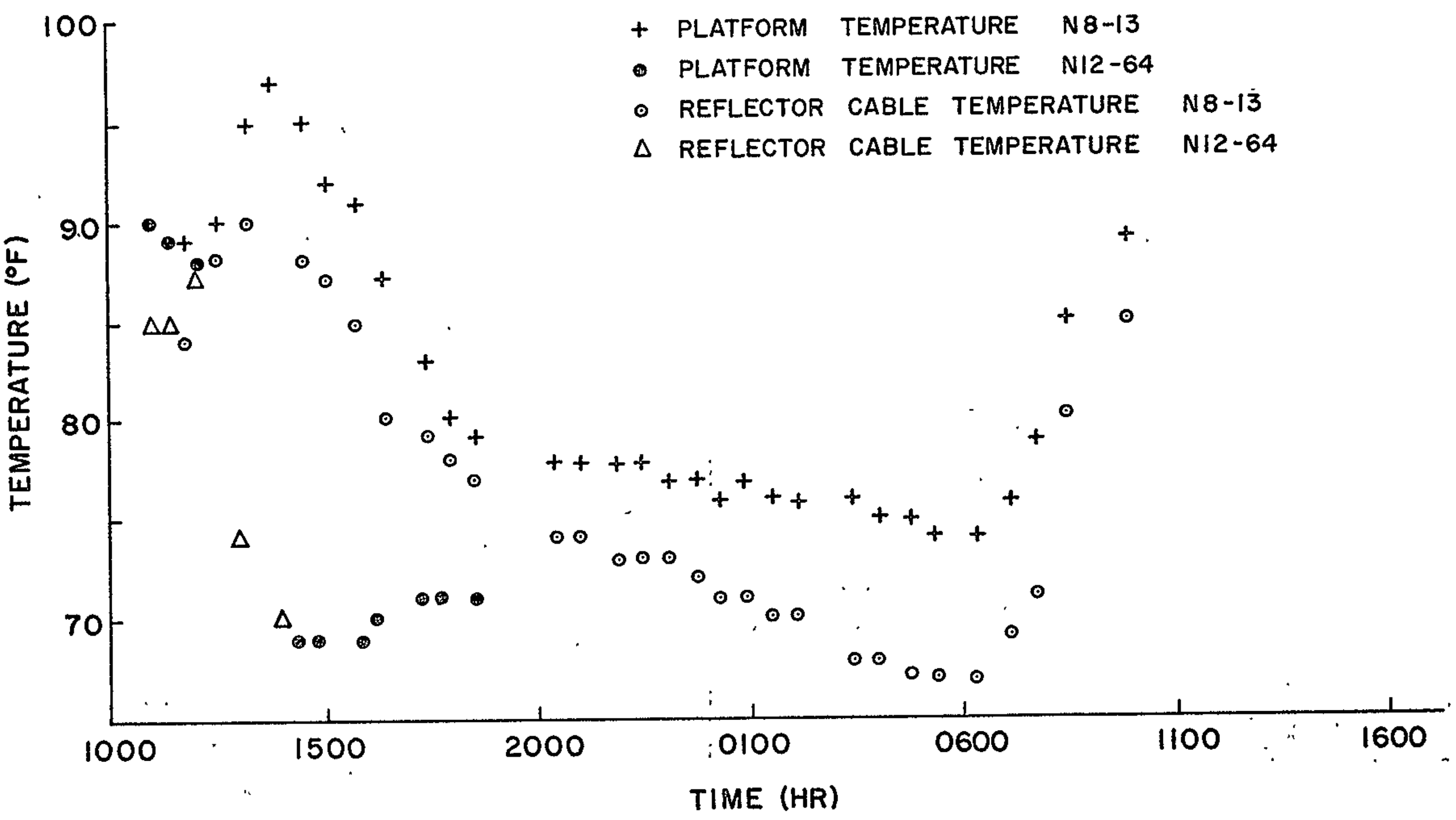

TEMPERATURE MEASUREMENTS

FIGURE 9

3.8 Backscatter Gain Calculations

Using Equations (1.5) and (2.3) backscatter gains were calculated for the December series of N11 ionospheric experiments. Measured values for the parameters in Equations (1.5) and (2.3) were taken at the peak. Figure 10 shows these gains plotted as a function of time. It can be seen that the plots for the N11-90 and N11-92 gains behave in a similar manner, reaching their maximum during the night and then starting to decrease at approximately 0600. The nighttime gains are approximately 1.75db greater than the daytime gains. The N11-91 backscatter gain plot is shifted downward from the other two plots by approximately 2db. It exhibits a day to night variation of approximately 1.2db.

Plots of backscatter gains versus time for gains calculated from N12 experiment data taken during the summer of 1968 are shown in Figure 11. The gains for the N12-42 experiment are approximately 1.75db higher during the night than during the day while N12-43 experiment backscatter gains are about 2.25db greater at night. For both experiments the gains began to decrease at 0700. Backscatter gains for the N12-45 experiment were calculated for a four hour period. The loss of the calibration pulse, as a result of a faulty Sanders switch, prevented further calculations. Still the day to night variation is exhibited during this period.

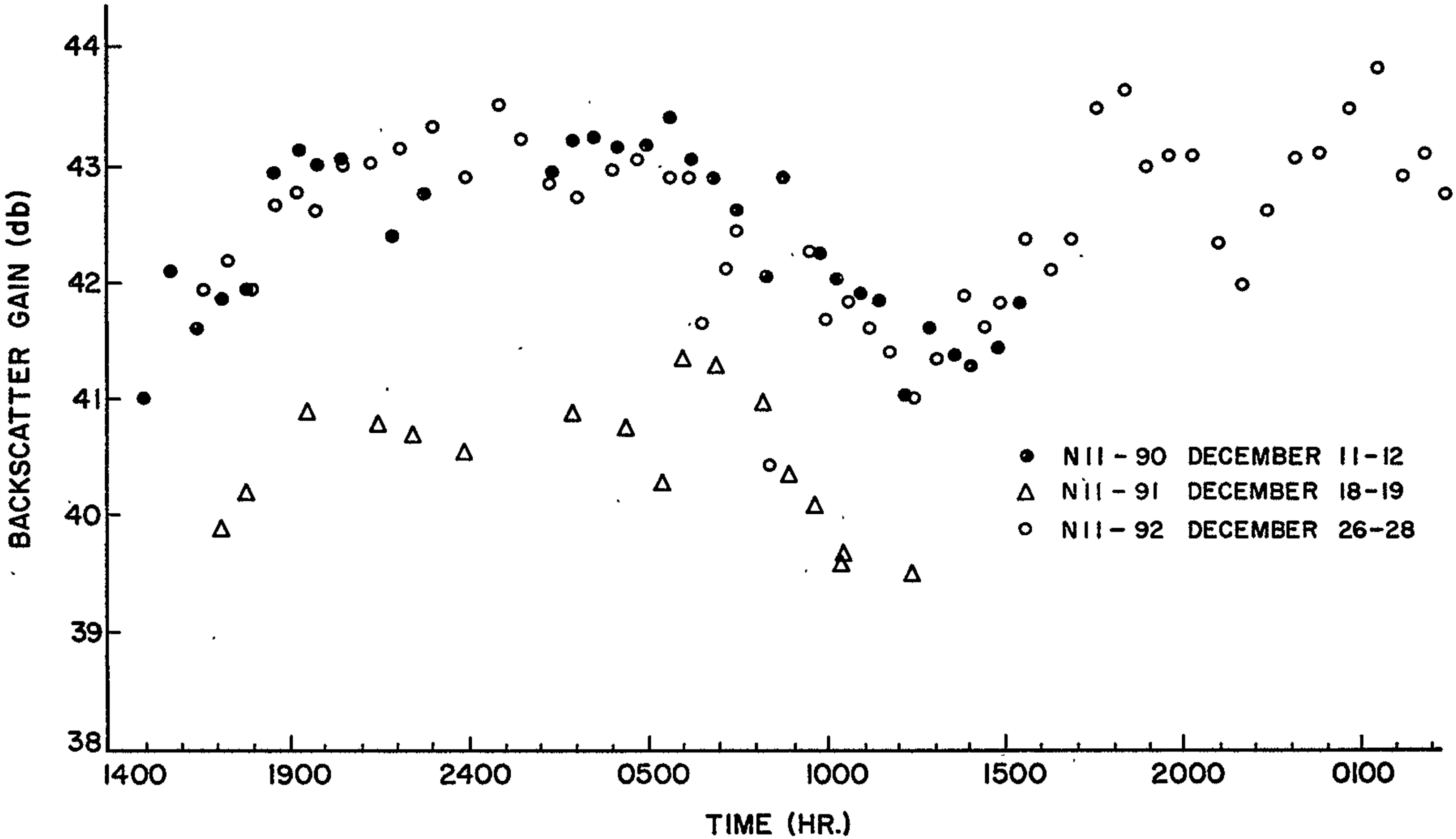

BACKSCATTER GAIN FOR DECEMBER 1967 N11 EXPERIMENTS

FIGURE 10

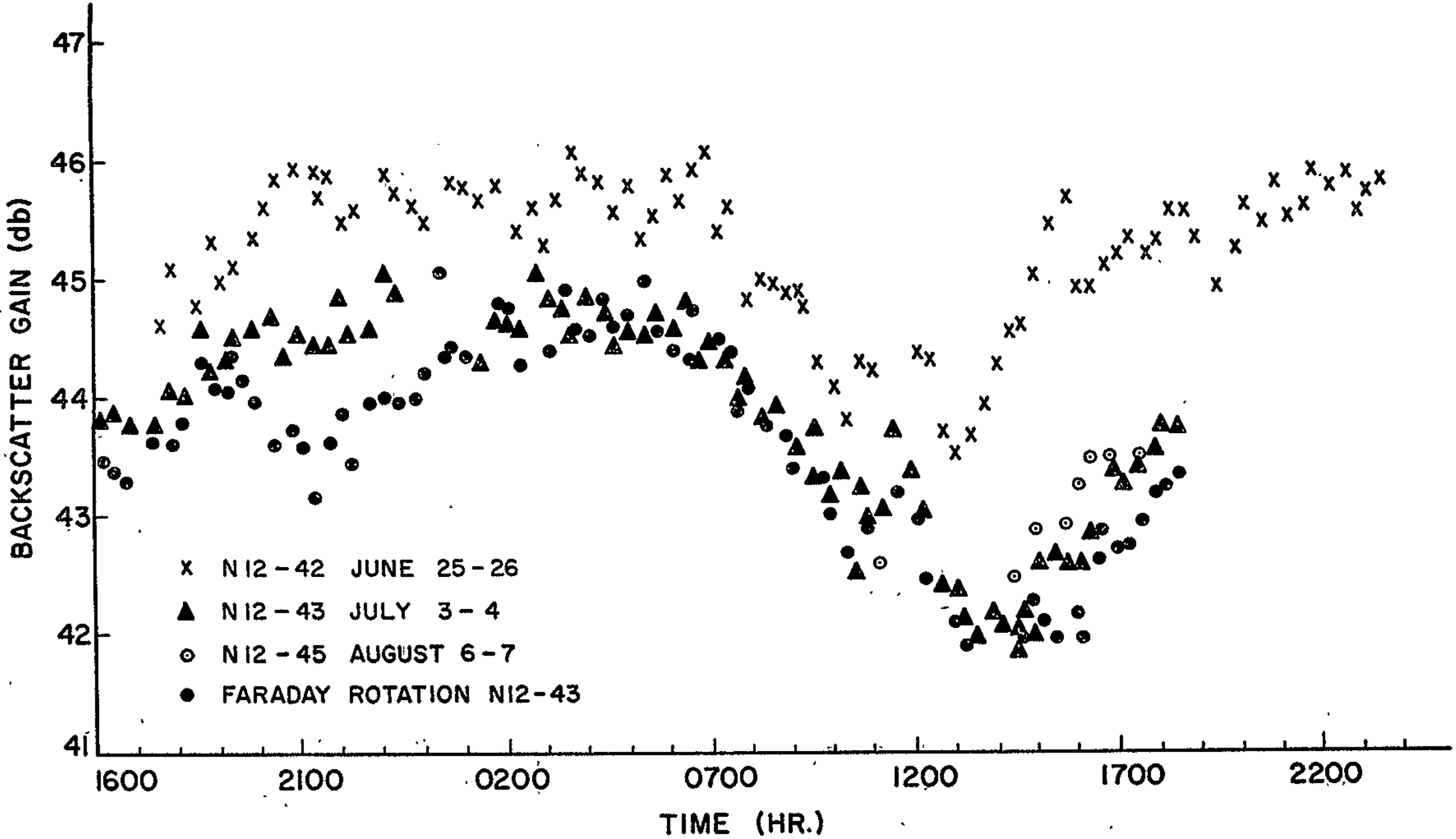

BACKSCATTER GAIN FOR SUMMER 1968 EXPERIMENTS

FIGURE 11

Backscatter gain versus time plots for the N12-52 and N12-54 experiments of December 1968 are shown in Figure 12. The N12-52 gains appear to be relatively constant over the 24 hour period. No gains were calculated for the period from 1700 to 0100, for the data was contaminated with equipment failures during that time. The N12-54 backscatter gains again demonstrate the day to night variations as seen previously. These gains are approximately 1.7db greater at night. There exists a difference between the N12-52 and N12-54 backscatter gains of about 2db.

It should be pointed out that the Sanders switch, which is used to introduce the noise calibration source into the system, burnt out during this series of experiments. It has been noted recently that the Sanders switch does introduce attenuation as it ages prior to burn out.

3.9 Noise Source Calibration Study

3.9.1 Study of the Noise Source Calibration Temperature

It can be seen from the backscatter gain versus time plots in Figures 11 and 12, that in addition to the diurnal backscatter gain variations, the backscatter gains for the N12-42 and N12-52 experiments are shifted by constants from the remaining N12 backscatter plots. To resolve this apparent discrepancy the temperatures of the noise calibration source were examined for these runs.

This was done by comparing the noise temperatures of the system for these runs. The system noise temperature includes the noise generated by the front end of the receiver plus the noise collected by the antenna from the

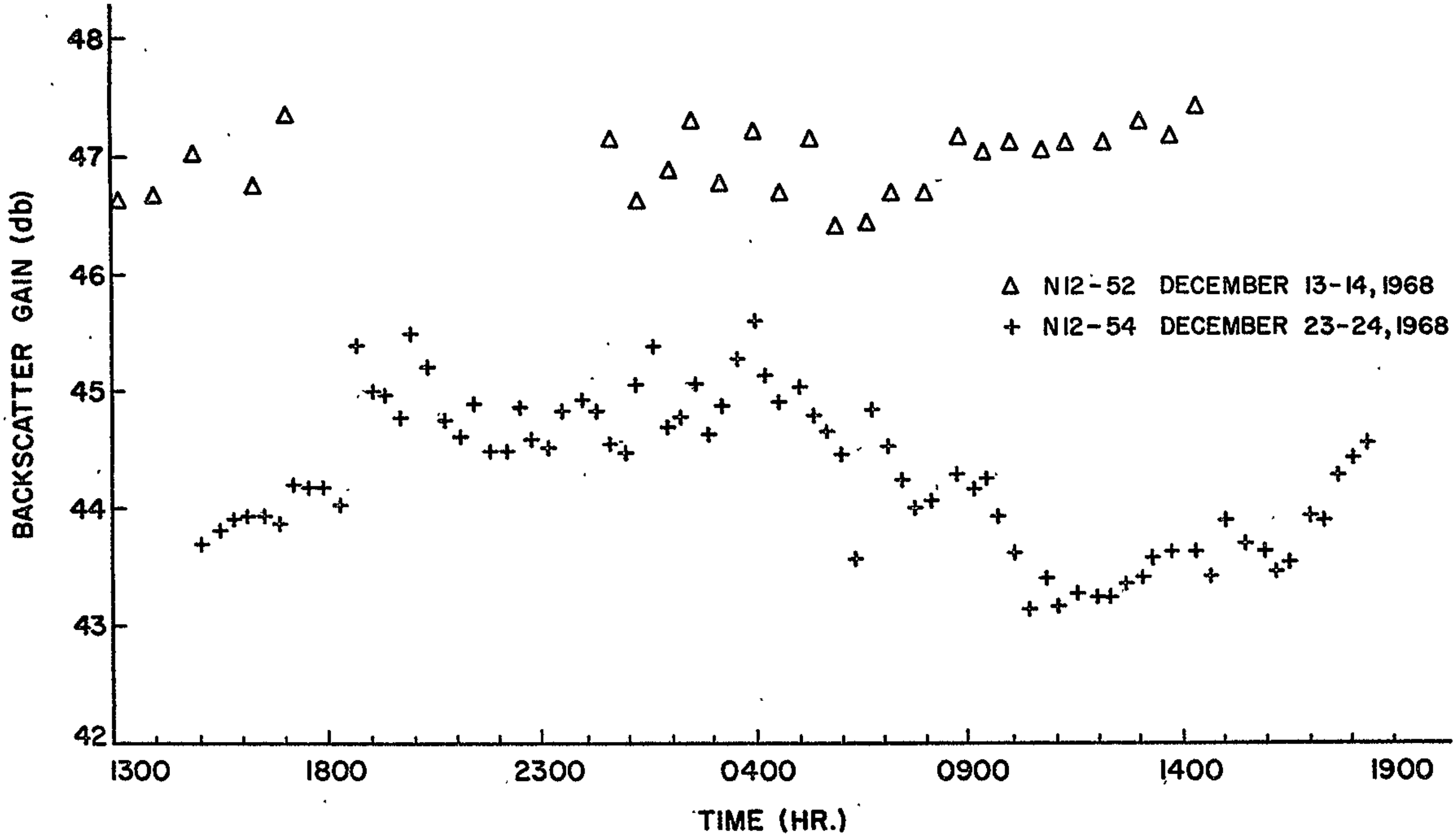

BACKSCATTER GAIN FOR DECEMBER 1968 EXPERIMENTS

FIGURE 12

sky background. The relative system noise temperature is calculated by the computer for each ionospheric run in the guise of the noise factor. Since

$$\text{noise factor} = \frac{\text{Relative system noise}}{\text{Relative calibration noise}}, \quad (3.8)$$

the absolute system noise temperature is simply the product of the noise factor times the noise calibration temperature. Upon comparing the system noise temperatures of the various runs it was discovered that while the system noise temperatures for experiments N12-43, N12-45, and N12-54 were all approximately 350°K, the system noise temperatures for experiments N12-42 and N12-52 were 450°K and 700°K respectively. In arriving at these figures care was taken to account for sky background variations.

The noise calibration temperatues for experiments N12-42 and N12-52 were corrected in accordance with the 350°K system noise temperature. Using these new calibration temperatures, corrected backscatter gain calculations were made. A plot of corrected backscatter gain versus time is shown in Figure 13. The good agreement of backscatter gains, as seen in Figure 13, implies that the noise calibration temperatures for experiments N12-42 and N12-52 were incorrect. As further proof it should be noted that the theoretical estimate of system noise temperature is 300°K. Considering sky background variations, the measured 350°K noise temperature is quite appropriate.

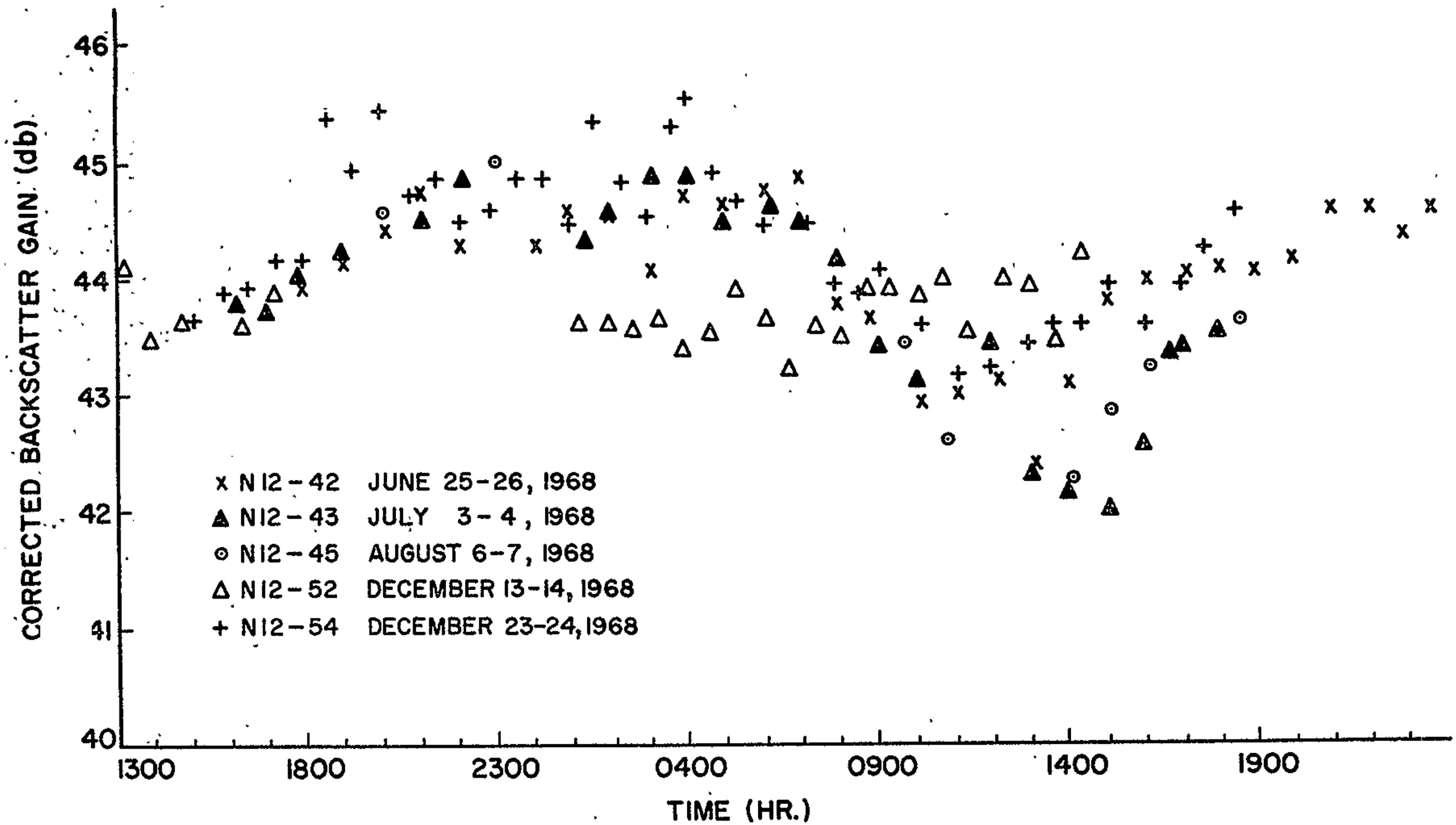

BACKSCATTER GAIN NORMALIZED USING SYSTEM TEMPERATURE

FIGURE 13

3.9.2 Diurnal Noise Source Stability

In order to determine the variability of the calibration pulse during an ionospheric experiment, differences between the calibration average and noise average were calculated for one N11 and three N12 type experiments. These differences, which are actually measures of the noise pulse, were averaged for all good runs of each experiment. Variations from the average were then determined.

The results of the calculations indicate that the average variations in the noise source are within ±5 percent. This figure includes variations which may result from receiver instability, sampling errors, and faulty switching equipment. Using the results of section 3.3, sampling errors were found to be ±1.5 percent. Thus, the results are in good agreement with the 7 percent variations as measured by Hardebeck (section 1.2.5). Though different noise sources were used, the experiments are in good agreement with respect to the variability of typical calibration sources.

3.10 Comparison of Backscatter Gains Calculated by the Various Methods

3.10.1 Ionosonde Data Versus Plasma Line Data

Since one of the parameters used in calculating the backscatter gain is the peak electron density, a comparison of backscatter gain calculations was made using peak electron densities obtained from ionograms, plasma lines, and Faraday rotation data. For the previous results presented in this paper only ionosonde data was employed to obtain the peak electron density.

It was given in section 1.2.3 that Perkins and Yngvesson calculated backscatter gains from plasma line data taken during October of 1966. The results of the calculations were that the backscatter gains were equal to 43.5 $\pm$.5db. Although the exact times for the measurements were not available, it is most likely that the measurements were made during the day when ionospheric conditions are suitable for plasma lines. For the N12-43 and N12-54 experiments the daytime backscatter gains were 42.82 $\pm$.7db and 43.59 $\pm$.5db respectively. Since the results of this paper indicate that the backscatter gains are dependent upon antenna reflector temperature, and since temperature measurements were not made for the plasma line experiment, it can only be said that the results as calculated by each method are in ballpark agreement.

3.10.2 Faraday Rotation Data Versus Ionosonde Data

Backscatter gains were calculated using Faraday rotation data obtained from the ATS-3 satellite. The Faraday rotation data was substituted for ionosonde date in order to obtain the peak electron density. This was done by noting that the Faraday rotation angle is given as

$$\Omega = \frac{F}{f^2} \int_0^{h_s} N B_L \sec\chi \, dh \qquad (3.9)$$

where Ω is the Faraday angle in radians

F is a constant equal to 2.36×10^4 rationalized MKS units

f is the satellite transmission frequency in HZ

N is the electron density

B_L is the induction of the earth's magnetic field multiplied by the cosine of the angle between the magnetic field and the raypath

χ is the zenith angle of the satellite

h_s is the height of the satellite

Since the electron density profile can be written as

$$N = N_p P, \tag{3.10}$$

where N_p is the electron density of the F2 peak

P is the normalized electron density profile

Equation (3.9) can be written in the form

$$\Omega = \frac{F N_p}{f^2} \int_0^{h_s} P B_L \sec\chi \, dh. \tag{3.11}$$

Equation (3.11) can be solved for N_p and the backscatter gains can be calculated after substitution into Equation (1.5) and (2.3).

For N12 type ionospheric experiments, the normalized profile is available for the height interval of 105km to 816km. Therefore to use Equation (3.10), approximations had to be used to account for rotations above and below the interval. For heights greater than 816km it was assumed that $(B_L\sec X)_{816}$ and $(N)_{816}$ each fall off as r^{-3}. Using Equation (3.9), the Faraday rotation from 816km to h_s was calculated to be

$$(\Omega)_{816-h_s} = 3.28 \times 10^{-4}(N)_{816} \qquad (3.12)$$

Since $(\Omega)_{816-h_s}$ must be known before Equation (3.11) can be solved, an initial guess must be made for $(N)_{816}$. Ionosonde data along with the normalized electron density profiles were emoloyed to make this guess. For Faraday rotations below 105km, Equation (3.9) was solved for h_s equal to 105km. Typical values for N were assumed for nighttime and daytime conditions. The results of the calculations showed that for the interval from 0 to 105km, Faraday rotations are approximately .22 degrees and 1.26 degrees for nighttime and daytime respectively.

Using the above approximations, Equations (1.5), (2.3), and (3.11) were employed to calculate backscatter gains for the N12-43 experiment. The results of these claculations are shown in Figure 11. In general backscatter gains as calculated using Faraday rotation data, exhibit a greater variation than those as calculated using ionosonde data.

3.11 Discussion of the Effect of Temperature Changes on the Backscatter Gain

Backscatter gain versus temperature plots for the N12-43, 45, and 54 experiments are shown in Figure 14. The temperatures are those recorded on the upper support cables of the reflector surface. Although some scatter is present, the plot does show a definite dependence of backscatter gain on temperature. A second degree polynomial was fit to these points and the result is the solid line in Figure 14. The average deviation of the measured backscatter gains from the curve is $\pm$.375db.

Figures 15 and 16 show backscatter gains for the N8-13 experiment plotted as a function of upper cable temperature and platform temperatures respectively. Again, the solid lines are the result of second degree polynomial least square fits to the measured data. It should be noted that while the curves are very similar in shape, the gain versus platform temperature curve is shifted to the right by approximately 4^{o}F. Also the average deviations of the measured data from the least fit curves are $\pm$.42db and $\pm$.38db for upper cable temperature dependence and platform temperature dependence respectively.

A case of special interest is the N12-52 experiment. From Figure 12 it can be seen that the backscatter gains show no diurnal variation as seen in the other gain plots. However, upon inspecting Figure 8 it is also realized that diurnal temperature variations for the day on which the experiment was run were less than 6^{o}F. Since both of these occurrences are exceptions, their coincidence offers strong substaniation to the previously described curves which show a backscatter gain temperature dependence.

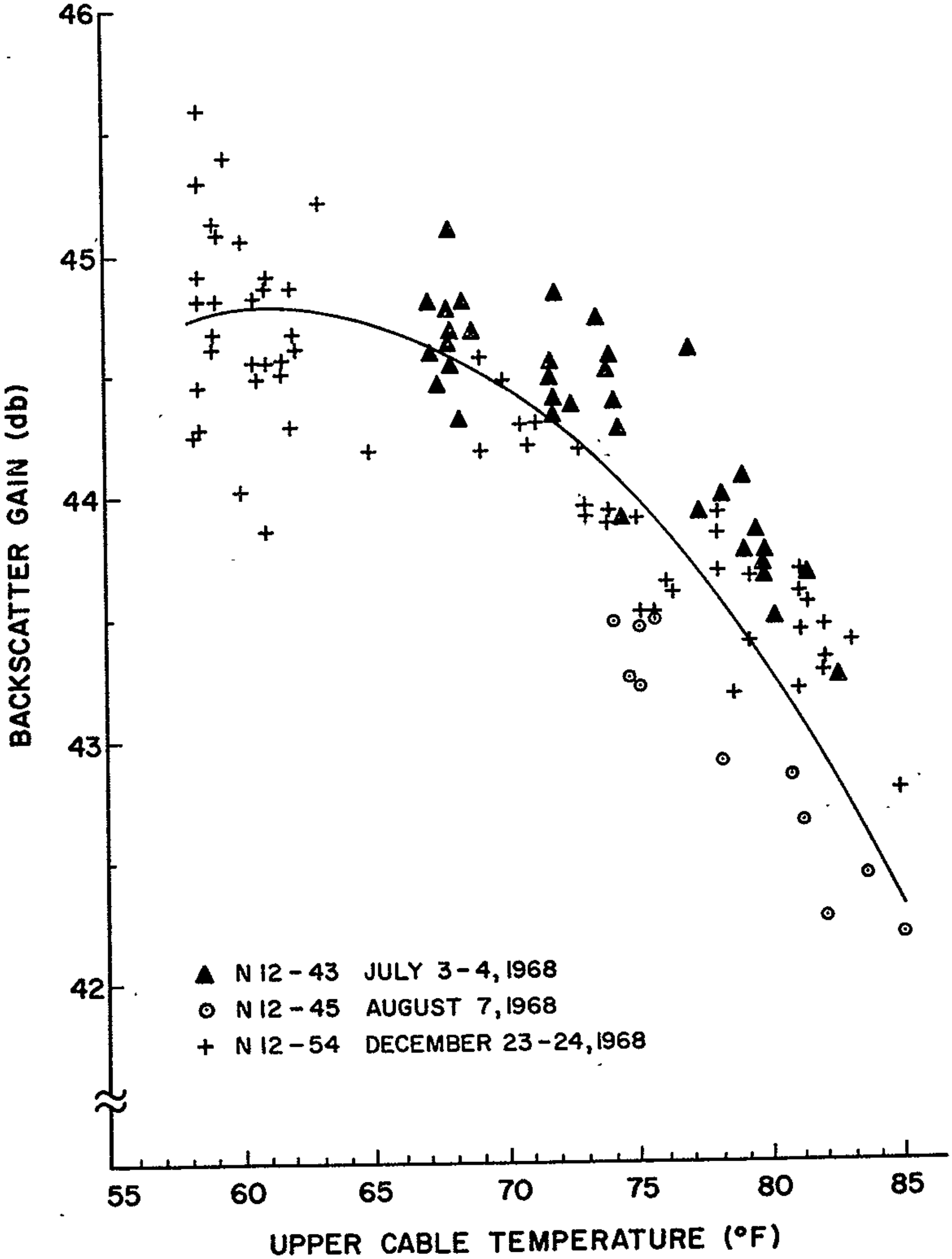

BACKSCATTER GAIN VS REFLECTOR TEMPERATURE

FIGURE 14

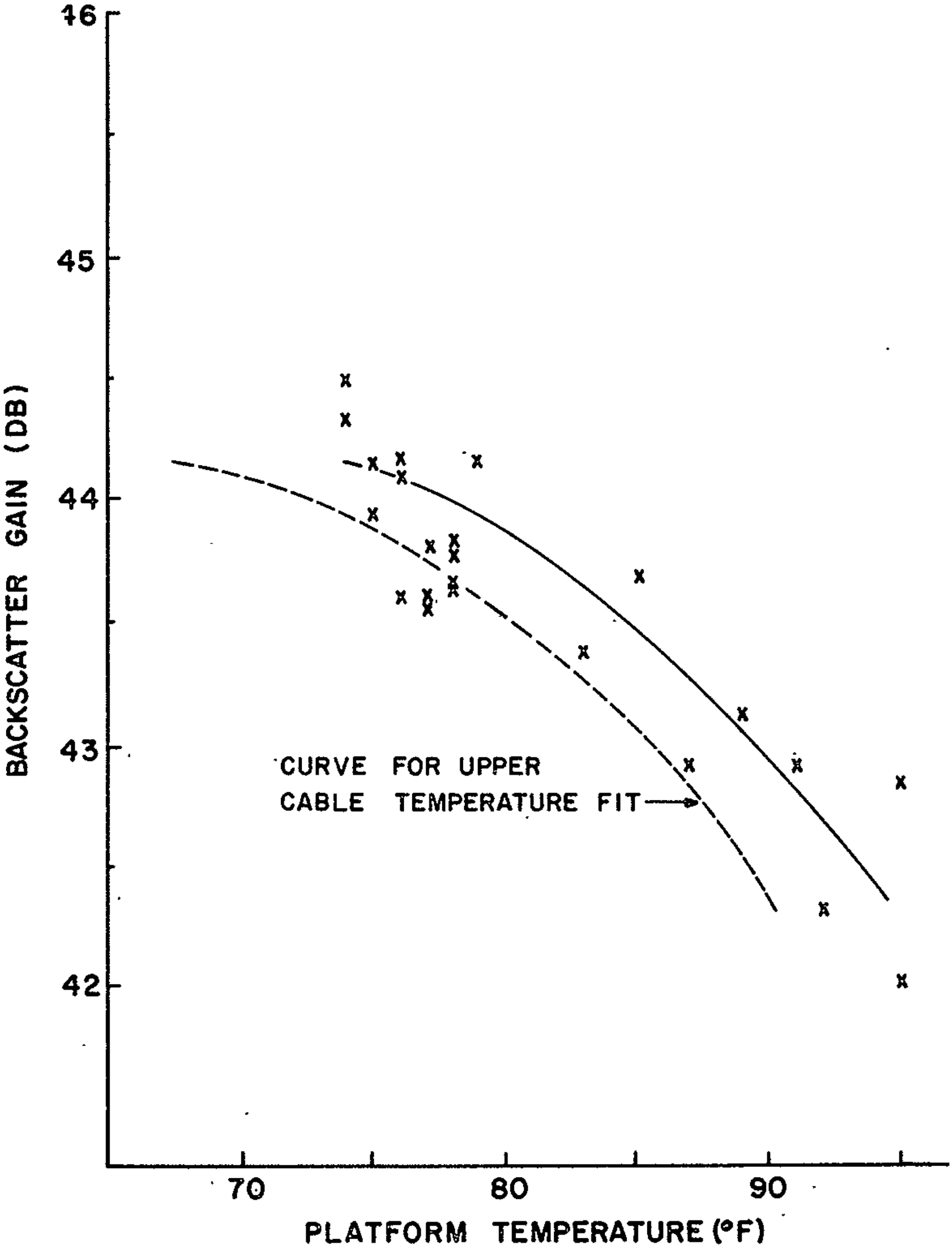

N8-13 BACKSCATTER GAINS

FIGURE 15

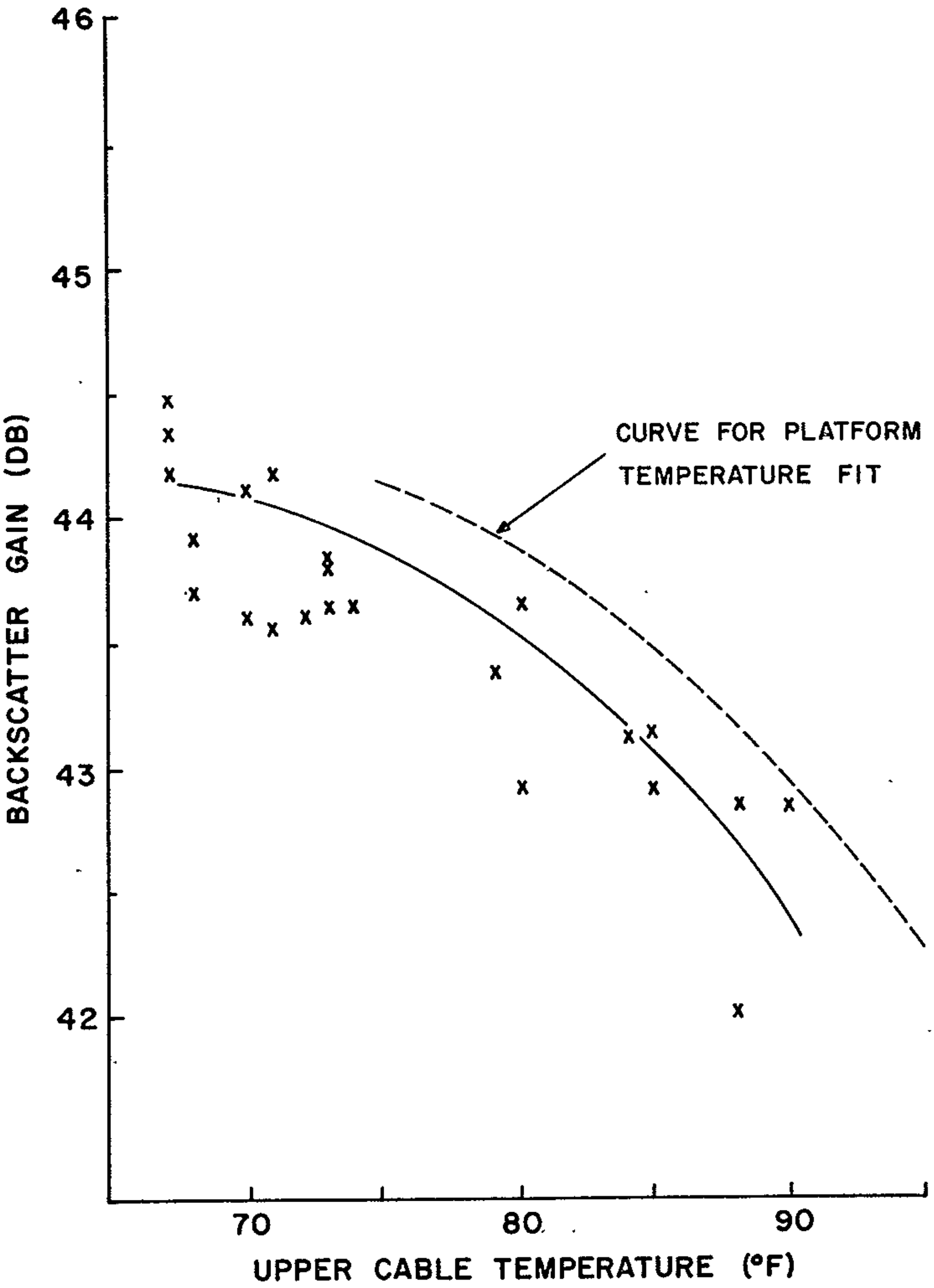

N8-13 BACKSCATTER GAINS

FIGURE 16

3.12. Theoretical Determination of Antenna Gain Fluctuations

3.12.1 Gain Degradations by Ruze

Ruze (1952) calculated statistically what effects bumps or warping of the reflector of a continuous aperture type antenna would have on the peak gain. For small deviations in the reflector surface the degradation in gain is due to phasing errors. Since an error at one point on the reflector surface might not be independent of an error at some other point, a correlation coefficient was introduced to account for the localization of errors. This coefficient is the distance at which the errors are independent of each other. For the case when the correlation coefficient is much greater than the wavelength, and when the errors are Gaussianly distributed, Ruze's relationship for gain degradiation reduces to

$$G_D = G_o \exp(-\overline{\delta^2}) \qquad (3.13)$$

where G_o is the designed gain of the perfect antenna

G_D is the degraded gain of the antenna as a result of phasing errors

$\overline{\delta^2}$ is the mean square phase error in radians on the surface of the aperture

Peak gain losses as a function of δ were calculated using Equation (3.13) and the results are shown in Figure 17.

3.12.2 Gain Losses by Numerical Methods

The maximum gain for a circular aperture antenna is given by Silver (1947) as

$$G_M = \frac{4\pi \left| \int_A A(r,\phi')e^{j\beta(r,\phi')} r dr d\phi' \right|^2}{\lambda^2 \left| \int_A \left[A(r,\phi')e^{j\beta(r,\phi')}\right]^2 r dr d\phi' \right|} \qquad (3.14)$$

and the normalized power pattern as given by Silver (1947)

$$p(\theta,\phi) = \left| \int_A A(r,\phi') \exp\left\{ j \left[\frac{2\pi a r}{\lambda} \sin\theta\cos(\phi') + \beta(r,\phi') \right] \right\} r dr d\phi' \right|^2 \qquad (3.15)$$

where r is the radial distance on the aperture

ϕ' is the azimuthal angle on the aperture

ϕ is the azimuthal angle measured with respect to a vertical plane containing the beam axis

θ is the polar angle measured from the beam axis

a is the radius of the aperture

λ is the wavelength

$A(r,\phi')$ is the amplitude variation on the aperture

$\beta(r,\phi')$ is the phase variation on the aperture

In order to utilize the above equations for gain calculations it is necessary to know $A(r,\phi')$ and $\beta(r,\phi')$. The design of the Arecibo antenna called for a 10db Gaussian taper amplitude distribution and a zero phase variation across the aperture. Although it is known that the above specifications were not realized in the fabrication of the antenna, the exact amplitude and phase variations are not well known. Some approximate results were obtained by LaLonde (1967), and these were used in the following calculations.

Using Equations (1.3), (3.14), and (3.15), the peak gains and backscatter gains were calculated numerically on the computer. The phase distribution was altered by introducing random Gaussianly distributed phase errors with standard deviation δ. The intervals used in the numerical integration were chosen so that each phase point represented approximately 100 square meters, for it is felt that at such distances the errors would be independent of each other. The peak gains and backscatter gains obtained from these calculations as a function of δ are plotted in Figure 17.

As should be expected, the peak gain degradation curves as calculated using Ruze's formula and the above method agree with each other. The backscatter gain degradation curve falls off approximatly twice as fast as the peak gain curve.

3.12.3 Applications of Gain Degradation Calculations to the Reflector Surface

It was shown in section 1.2.6 that Forrest and Philipson made reflector surface studies in which the standard deviations of the reflector surface from a best fit sphere were measured and calculated at various temperatures. These displacement errors on the surface were converted to phase errors on the aperture and upon applying

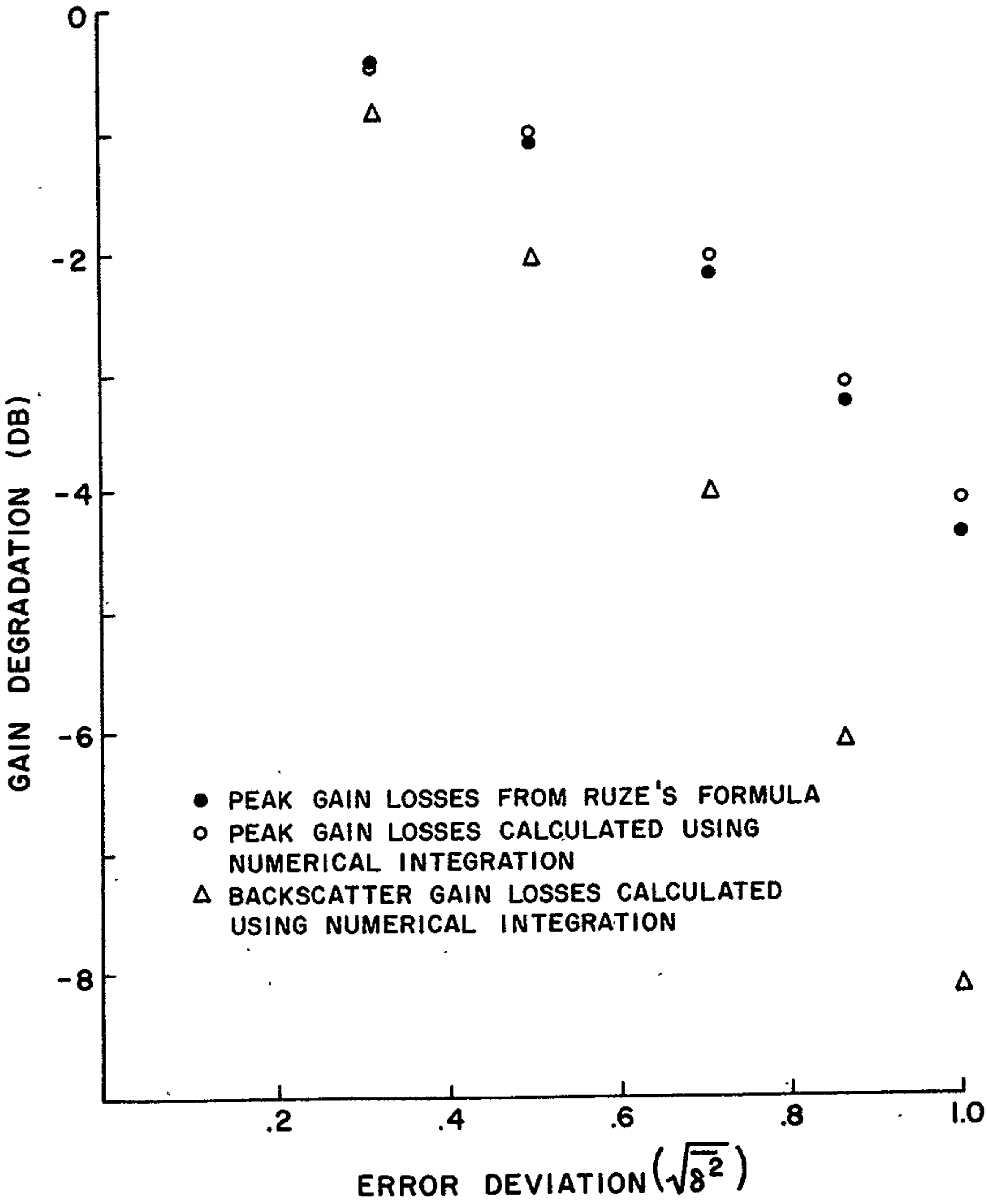

GAIN DEGRADATION CALCULATIONS

FIGURE 17

the results given in section 3.12.2, the backscatter gain degradation as a function of temperature was obtained. These results are plotted in Figure 18 along with the averaged measured gain degradation from the N12-43, N12-45, and N12-54 experiments.

3.12.4 Gain Degradations for Line Feed Motion and Reflector Radius Change

Displacement of the line feed and reflector radius change, which in effect acts as a feed displacement, cause phase errors on the antenna aperture which are given by

$$\nabla \emptyset = \frac{2\pi\epsilon}{\lambda} \cos 2\psi \qquad (3.16)$$

where ϵ is the displacement of the line feed from its optimum position

ψ is the angle between an incident ray and a line drawn to the center of the spherical reflector from the point of reflection ($0 \leq \psi = 35^{\circ}$).

The reflector radius changes with temperatures were measured by Philipson and are given in section 1.2.6. The line feed displacement is known to be .33cm per degree Fahrenheit. The effects are compensating and for a 30°F temperature change, the effective displacement, ϵ, was calculated to be 8cm. Using this value in Equation (3.16) and then incorporationg this phase error into Equations (1.3), (3.12), and (3.15), the peak and backscatter gains were calculated. The results of these calculations showed that

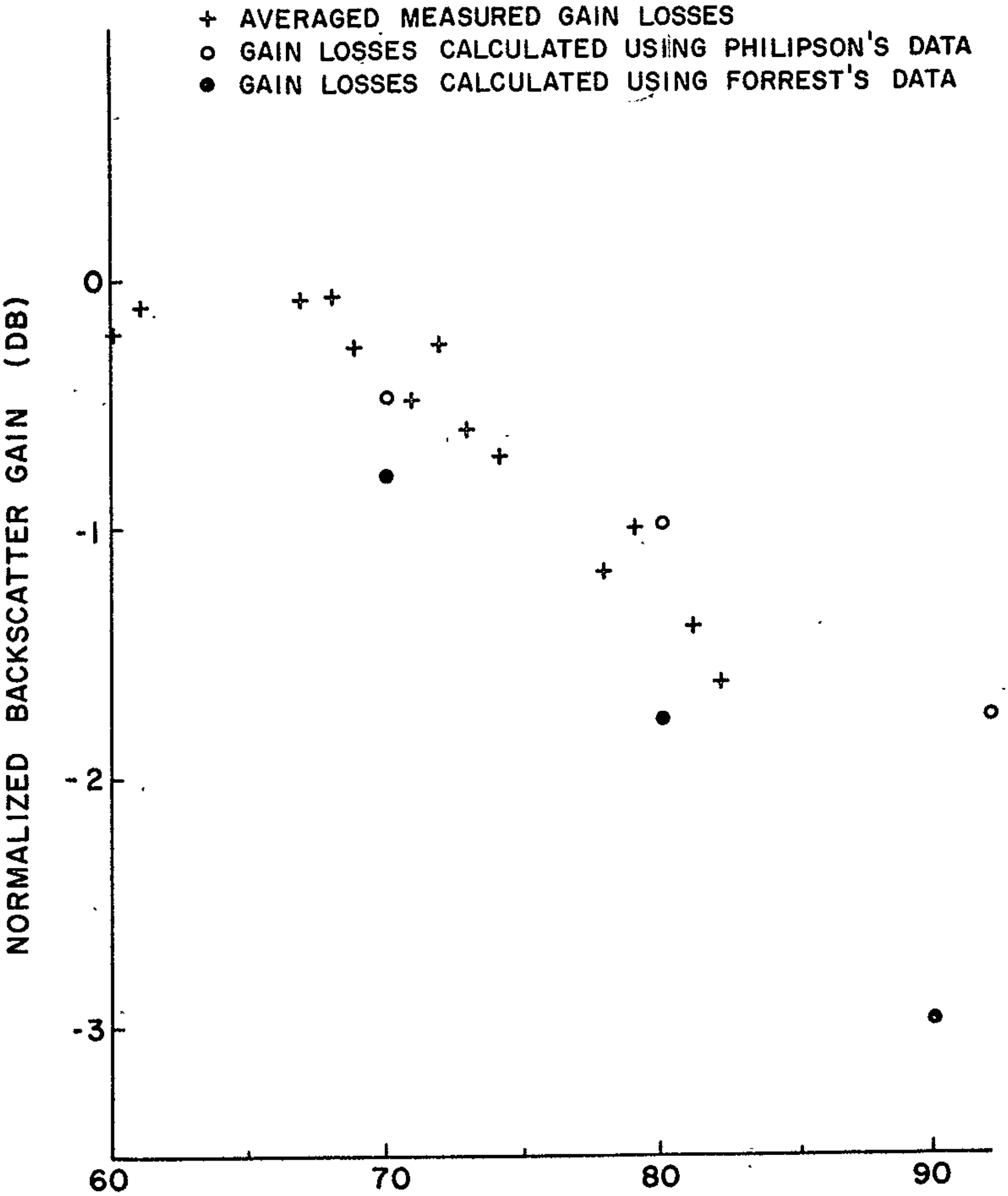

BACKSCATTER GAIN LOSS CALCULATIONS
FIGURE 18

peak gain and backscatter gain variations were less than .05db for the displacement caused by the 30°F temperature variations.

3.12.5 Considerations for the Previous Calculations

The absolute backscatter gains and absolute peak gains calculated in section 3.12.2 are approximately 6db greater than the respective measured gains. The reason for this disagreement is that the amplitude and phase distributions used were not sufficiently accurate in that they do not account for the underilluminated sections of the reflector. Since the prime interest is the change in backscatter and peak gains resulting from phase errors, and since it was not known how phase errors would affect the backscatter gain and peak gain of an underilluminated antenna, the amplitude distribution function used in section 3.12.2 was modified in order to account for underilluminated areas. Thus the absolute backscatter gain and peak gain were forced to agree with the measured values. However, the gain degradation curves calculated for the underilluminated antenna remained practically the same as those given in Figure 17. The conclusion here is that even though absolute gain of the antenna is greatly affected by underillumination of the reflector, degradations in the gain as a result of phase errors affect the properly illuminated and underilluminated antenna approximately equally.

CHAPTER IV

CONCLUSIONS

The results of this study are as follows:

1. Backscatter gains were found to vary from 42.0db to 45.5db and on the average follow the realtionship

$$\overline{G} = (28.49 + .53T - .0043T^2) \pm .4db \qquad (4.1)$$

   where T is the upper reflector cable temperature ^{o}F $(55 \leq T \leq 100)$. The primary cause of the variations were concluded to be distortions in the antenna reflector surface as a result of the temperature changes. Inaccuracy of the parameters of Equation (1.1) caused statistical variations of a standard deviation of $\pm$.4db.

2. The accuracy of the basic parameters (P_T, P_R, σ, R) determined in the area of the F2 peak have a direct reflection on the accuracy of the electron density. Inaccuracies in the measurements of the power transmitted were found to be lower than the measurement threshold of the experiments conducted. Errors in determining the power returned were within $\pm$8 percent whereas errors in determining the observed electron cross section and height of the F2 peak were found to be $\pm$4 percent and $\pm$3 percent respectively.

3. Backscatter gains as calculated using plasma line data Faraday rotation data, and ionosonde data were found to agree within the limits of the measured gain variations. Ionosonde data, used in conjunction with normalized electron density profiles obtained from the incoherent backscatter sounder, were found to be most suitable for determining the backscatter gains when the ionograms were good. Faraday rotation angles were found to be easily obtained, however, the use of this data requires that the entire normalized electron density profile be accurate. Plasma line data yielded good backscatter gain results, but this data in unavailable under nighttime conditions when the conjugate region is in darkness.

4. Backscatter gain variations can best be reduced by improvement of the reflector surface with regard to surface deviations. Corrections for backscatter gain variations using the present surface can usefully be made using temperature measurements and Equation (4.1).

BIBLIOGRAPHY

Buneman, O., "Scattering of Radiation by the Fluctuations in a Nonequilibrium Plasma", J. Geophys. Res., 67, No. 5, pp. 2050-2053, 1962

Dougherty, J. P. and D. T. Farley, "A Theory of Incoherent Scattering of Radio Waves by a Plasma", Proc. Roy. Soc., A259, pp. 79-99, 1960.

Dougherty, J. P. and D. T. Farley, "A Theory of Incoherent Scattering of Radio Waves by a Plasma III: Scattering in a Partly Ionized Gas", J. Geophys. Res., 68, No. 19, pp. 5473-5486, 1963.

Evans, J. V., "Design Considerations for a Thomson Scatter Radar", Aeronomy Report No. 17, University of Illinois, pp. 42-59, 1967.

Evans, J. V., "Electron Temperature and Ion Composition in the F1 Region", J. Geophys. Res., 72, No. 13, pp. 3343-3355, 1967.

Farley, D. T., "A Theory of Incoherent Scattering of Radio Waves by a Plasma IV: The Effect of Unequal Ion and Electron Temperatures", J. Geophys. Res., 71, No. 17, pp. 4091-4098, 1966.

Fejer, J. A., "Scattering of Radiowaves by an Ionized Gas in Thermal Equilibrium", Can. J. Phys., 38, No. 8, pp. 1114-1133, 1960.

Fejer, J. A., "Scattering of Radiowaves by an Ionized Gas in Thermal Equilibrium in the Presence of a Uniform Magnetic Field", Can. J. Phys., 39, No. 5, pp. 716-740, 1961.

Forrest, R. B., "Calibration of the 1000 foot Arecibo Radio Reflector", Research Report CRSR 204, Cornell University, pp. 1-54, 1965.

Gordon, W. E., "Incoherent Scattering of Radiowaves by Free Electrons with Application to Space Exploration by Radar", Proc. I.R.E., 46, No. 11, pp. 1824-1829, 1958.

Hardebeck, H. E., "Antenna Calibrations Using Radio Sources", Research Report RSG 5, Cornell University, pp. 1-49, 1965.

LaLonde, L. M., "Minutes of Meeting Arecibo Feed Subpanel", Lincoln Laboratory, MIT, Appendix V, pp. 1-7, 1967.

Moorcroft, D. R., "On the Determination of Temperatures and Ionic Composition by Electron Backscattering from the Ionosphere and Magnetosphere", J. Geophys. Res., 69, No. 5, pp. 955-970, 1964.

Nisbet, J. S., "On the Construction and Use of Simple Ionospheric Models", Radio Sci., in print, 1970.

Perkins, F. W. and E. E. Salpeter, "Enhancement of Plasma Density Fluctuations by Non-thermal Electrons", Phys. Rev., 139A, No. 139, pp. 59-62, 1965.

Perkins, F, W., E. E. Salpeter and K. O. Yngvessan, Incoherent Scatter from Plasma Oscillations in the Ionosphere", Phys. Rev. Letter, 14, No. 15, pp. 579-581, 1965.

Perkins, F. W. and R. Wand, "Analysis of the Ionosphere Incoherent Scatter Signal by Digital Methods", Research Report CRSR 207, Cornell University, pp. 1-47, 1965.

Petit, M., "Application de la Diffusion << Quasi-incohérent >> a la Mesure de la Température, de la Composition Ionique et de la Concentration Électronique de L'Ionosphère", Ann. de Geophys., 19, No. 1, pp. 63-70, 1964.

Phillipson, W. R., "Geometric Calibration of Arecibo One Thousand Foot Reflector", M.S. Thesis, Cornell University, pp. 1-204, 1968.

Ruze, J., "Physical Limitations on Antennas", Tech. Rept., No. 248, MIT Research Lab. Electronics, pp. 1-82, 1952.

Salpeter, E. E., "Electron Density Fluctuations in a Plasma", Phys. Rev., 120, No. 5, pp. 1528-1535, 1960a.

Salpeter, E. E., "Scattering of Radiowaves by Electrons Above the Ionosphere", J. Geophys. Res., 65, No. 6, pp. 1851-1852, 1960b.

Silver, S., "Microwave Antenna Theory and Design", Radiation Laboratory Series, 12, 1947.

Thome, G. E., "Some Antenna Characteristics", Private Communication, 1963.

Thomson, J. J., "Conduction of Electricity Through Gases", University Press, Cambridge, p. 321, 1906.

Warner, R. E., Private Communication, 1967.

Yngvesson, K. O. and F. W. Perkins, "Ionosphere Radar Equation", Private Communication, 1966.